AD-A114 987 S H E CORP SAN DIEGO CA F/G 13/1
PRELIMINARY STUDY OF A REGENERATIVE CYCLE CRYOCOOLER TO REACH 5--ETC(U)
AUG 80 R E SAGER N00014-80-C-0463
UNCLASSIFIED SHE-80-68001-1 NL

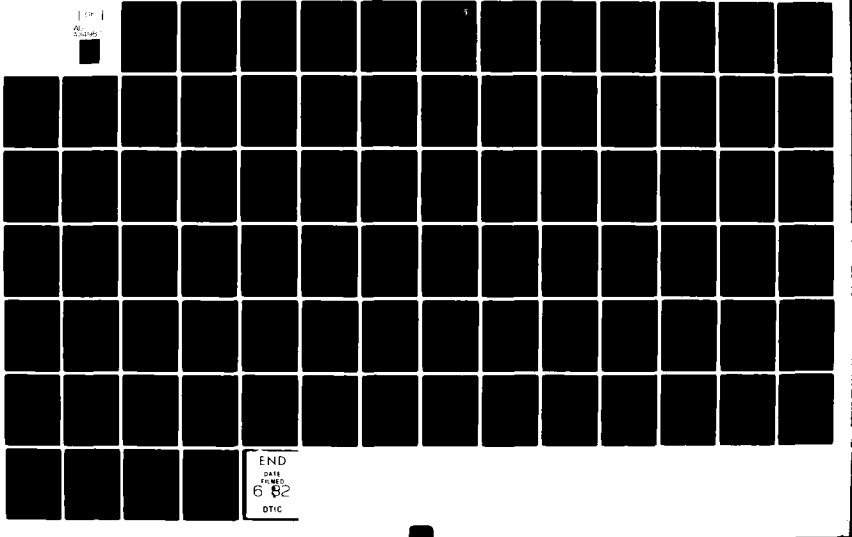

END
DATE FILMED
6 82
DTIC

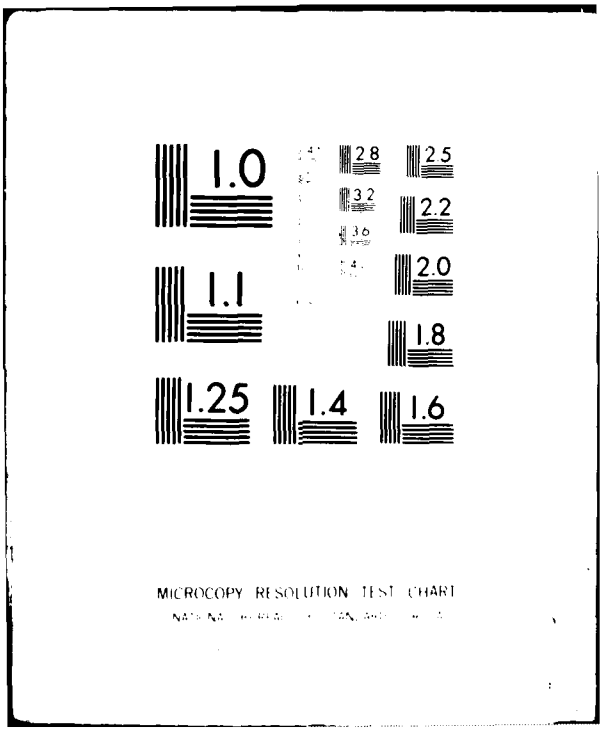
1.0
1.1
1.25
2.8
3.2
3.6
4.0
2.5
2.2
2.0
1.8
1.4
1.6
MICROCOPY RESOLUTION TEST CHART

NR 410-004
(1) Cab

AD A114987

DTIC FILE COPY

82 05 28 054

S-E CORPORATION

(1)cab

S.H.E. CORPORATION CRYOGENIC INSTRUMENTS AND SYSTEMS

May 13, 1980

Mr. Edgar A. Edelsack
Office of Naval Research
Physical Sciences Division (Code 420)
800 N. Quincy Street
Arlington, VA 22217

File

MR 4/10-007

Contract #N00014-80-C-0463

Dear Ed:

With regard to our conversation of 5 May, I'm submitting our mid-contract progress report (Contract #N00014-80-C-0463) to provide you with a general description of our progress to date and what we yet hope to achieve. Our approach to the problem has been oriented toward first understanding the work that Zimmerman has recently performed, then building on that basis using our own innovations.

We have devoted the first three and one half weeks of the contract (through May 12, 1980) primarily to the study of a simple multistage Stirling cryocooler with displacer and walls consisting of nylon. To date, our work has followed roughly in the footsteps of Zimmerman who has achieved a temperature of about 8 Kelvin with a similar type of device.

During this period we have investigated in some detail the regeneration loss, the shuttle heat loss, and the loss through axial heat conduction to be expected in a machine of this type. These calculations have produced first order estimates of the thermal loading for each stage of the machine and a "zeroth order" estimate for the dimensions (diameter and length) of each stage of a hypothetical Stirling cooler. It is interesting to note that, while our initial estimates for the engine parameters were based strictly on our calculated regeneration, conduction, and shuttle losses, the lengths and diameters of the various stages are rather similar to those actually used by Zimmerman in his cryocooler.

4174 SORRENTO VALLEY BLVD. | SAN DIEGO, CA 92121 | TEL: (714) 453-6300 | TELEX: 697903

With the understanding we have gained thus far, we feel that we now understand quantitatively, and can solve, the fundamental problems which limit the performance of this type of machine. In our "zeroth order" design, heat conduction down the displacer and walls severely limits the excess refrigeration available at the first two stages of the machine; in the third stage regeneration and conduction are the most important loss mechanisms, and in the final stage regeneration loss completely dominates all other thermal losses.

Following the ideas presented in our original proposal, we are now in the process of estimating expected improvements in the cryocooler performance when the two coldest stages of the displacer are loaded with helium to increase the heat capacity of the regenerating material. In addition, we are considering means of reducing the conduction losses in the warmer stages of the machine.

The enclosure shows our progress in the context of the overall work which we originally hoped to address during the course of this contract. There are seven areas we proposed to deal with:

1. Identification of materials to be used in the engine

2. Estimates of refrigeration requirements at each stage of the cryocooler

3. Performance calculations for a helium loaded regenerator in a Stirling cryocooler

4. Improvement in Stirling c[illegible]er performance when using ^{3}He as the work[illegible]id

5. Preliminary outline of a mechanical system to drive the displacer and provide the required pressure changes in the engine

6. Preliminary outline of measurements to determine magnetic and electrical signatures and noise in the cryocooler, and

7. Evaluation of the necessity for including a Malone stage in the design and a preliminary

estimate of its performance if the Malone stage is required.

The enclosure shows our estimated timetable for completion of the various aspects of the study; the open triangles indicate our current progress. A major part of our calculational effort (as expected) has gone into deriving expressions for the performance and design of a multistage Stirling machine in terms of the thermodynamic properties of the working fluid and the regenerator. This work has been essentially completed and we are now incorporating the appropriate modifications to estimate the effects of a helium loaded regenerator and the use of ^{3}He as the working fluid.

To date, our work has progressed roughly as expected, however, based on our initial calculations, it now appears that the Malone stage will not be required. Consequently, the time which we had previously allocated for investigating the Malone cycle will probably be devoted to a more detailed look at using ^{3}He as the working fluid and at providing a mechanical structure at the cold end of the engine with which to thermally couple the engine to some type of cryogenic apparatus. At this point we anticipate no substantial difficulty in meeting the remaining requirements of the contract.

Sincerely,

Ronald E. Sager

Ronald E. Sager
Principal Investigator

RES/dmo

Encls.

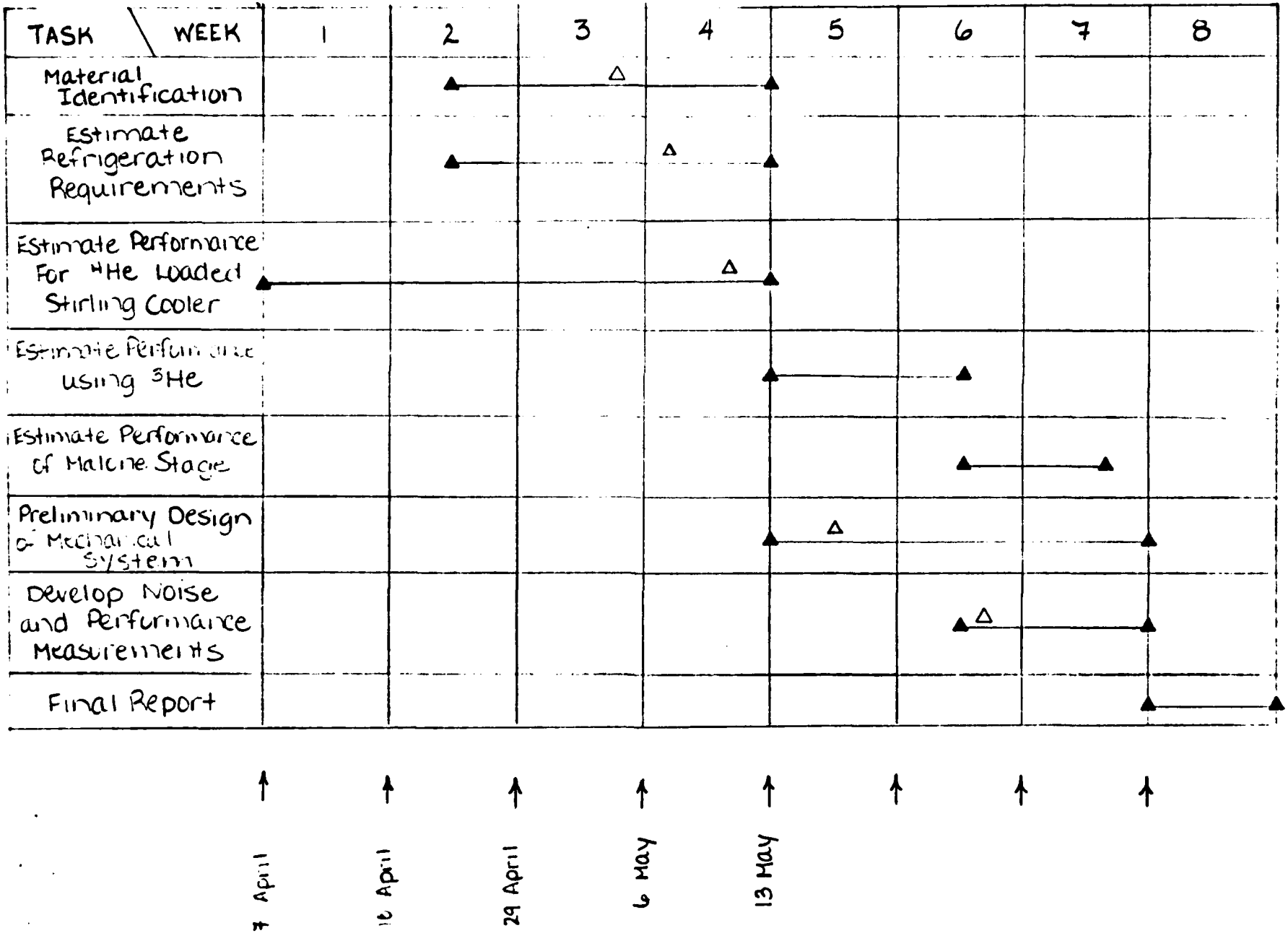
TASK
WEEK
1
2
3
4
5
6
7
8
Material Identification
Estimate Refrigeration Requirements
Estimate Performance For ⁴He Loaded Stirling Cooler
Estimate Performance using ³He
Estimate Performance of Machine Stage
Preliminary Design of Mechanical System
Develop Noise and Performance Measurements
Final Report
7 April
29 April
6 May
13 May

PRELIMINARY STUDY OF A REGENERATIVE CYCLE CRYOCOOLER TO REACH 5.0 KELVIN

FINAL REPORT

ONR CONTRACT No. N00014-80-C-0463

S.H.E. CORPORATION
CRYOGENIC INSTRUMENTS AND SYSTEMS
4174 SORRENTO VALLEY BLVD.
SAN DIEGO, CA 92121

TEL (714) 453-6300 TELEX 697903

Report SHE-80-68001-1

PRELIMINARY STUDY OF A REGENERATIVE CYCLE CRYOCOOLER TO REACH 5.0 KELVIN

Ronald E. Sager
S.H.E. Corporation
4174 Sorrento Valley Blvd.
San Diego, CA 92121

29 August 1980

Final Report for 1 April to 19 August 1980

Prepared For:

OFFICE OF NAVAL RESEARCH
800 North Quincy Street
Arlington, VA 22217

Defense Contract Administration Services
Management Area - San Diego
Bldg 4, AF Plant 19
4297 Pacific Hwy
San Diego, CA 92110

UNCLASSIFIED

SECURITY CLASSIFICATION OF THIS PAGE (When Data Entered)

REPORT DOCUMENTATION PAGE		READ INSTRUCTIONS BEFORE COMPLETING FORM
1. REPORT NUMBER SHE-80-68001-1	2. GOVT ACCESSION NO.	3. RECIPIENT'S CATALOG NUMBER
4. TITLE (and Subtitle) Preliminary Study of a Regenerative Cycle Cryocooler to Reach 5.0 Kelvin		5. TYPE OF REPORT & PERIOD COVERED Final Report for 1 April 1980 to 29 Aug 1980 6. PERFORMING ORG. REPORT NUMBER
7. AUTHOR(s) Ronald E. Sager		8. CONTRACT OR GRANT NUMBER(s) ONR Contract Number N00014-80-C-0463
9. PERFORMING ORGANIZATION NAME AND ADDRESS S.H.E. Corporation 4174 Sorrento Valley Blvd. San Diego, CA 92121		10. PROGRAM ELEMENT, PROJECT, TASK AREA & WORK UNIT NUMBERS
11. CONTROLLING OFFICE NAME AND ADDRESS Office of Naval Research 800 North Quincy Street Arlington, VA 22217		12. REPORT DATE 29 August 1980 13. NUMBER OF PAGES 77
14. MONITORING AGENCY NAME & ADDRESS(if different from Controlling Office) Defense Contract Administration Services Management Area - San Diego Bldg 4, AF Plant 19, 4297 Pacific Hwy. San Diego, CA 92110		15. SECURITY CLASS. (of this report) Unclassified 15a. DECLASSIFICATION/DOWNGRADING SCHEDULE

16. DISTRIBUTION STATEMENT (of this Report)

~~To Be Determined by Scientific Officer~~

17. DISTRIBUTION STATEMENT (of the abstract entered in Block 20, if different from Report)

Same As Item 16

18. SUPPLEMENTARY NOTES

19. KEY WORDS (Continue on reverse side if necessary and identify by block number)

Cryocooler, Stirling Cycle, Regeneration Loss, Shuttle Loss, Displacer

20. ABSTRACT (Continue on reverse side if necessary and identify by block number)

The ultimate low temperature achieved by a cryocooler is determined by the balance between its intrinsic refrigeration power and its thermal losses. This study examines in detail the thermal losses which occur in a regenerative cycle cryocooler and estimates the low temperature limit for a proposed cryocooler design. The study also discusses possible mechanical systems for providing motive power and the compression and expansion processes required for the refrigeration cycle.

DD FORM 1 JAN 73 1473 EDITION OF 1 NOV 65 IS OBSOLETE
S/N 0102-LF-014-6601

UNCLASSIFIED

SECURITY CLASSIFICATION OF THIS PAGE (When Data Entered)

TABLE OF CONTENTS

TABLE OF CONTENTS (Con't)

LIST OF FIGURES AND TABLES

LIST OF FIGURES AND TABLES (Con't)

ACKNOWLEDGMENTS

I would like to acknowledge the participation in this work of Professor John C. Wheatley who, as a consultant, provided substantial guidance and many valuable ideas, as well as establishing the groundwork for our proposed cryocooler program. I would also like to thank Dr. Ray Sarwinski for his computations regarding the radiation losses to be expected in the cryocooler, and Dr. Michael Simmonds for his many useful conversations and suggestions. Finally I would like to thank Miss Jackie Gallegos for her patience and untiring efforts in typing this report.

I. INTRODUCTION

During the period of this contract we have attempted to understand the fundamental principles of a cryocooler working on the Stirling principle. Although S.H.E. Corporation has had extensive experience in the design and construction of cryogenic apparatus, our knowledge of mechanical low-temperature refrigerators was rather limited. As a result, we began our investigation from a rather basic level; in particular, we first asked, "What are the sources of thermal loss which place fundamental limitations on the low-temperature performance of mechanical cryocoolers?"

In answering this question, we have estimated probable thermal losses from a variety of mechanisms which clearly have the effect of transporting heat into the cold end of the machine. We devoted the first part of our investigation to a description of thermal transfer associated with regeneration loss and shuttle heat loss in a cylindrical geometry, and after deriving general expressions for these mechanisms, we applied the equations to three different cases. The first was a machine similar to Zimmerman's[1] in which the displacer and cylinder walls, which also serve as the regenerator, were made of plastic. The second case incorporated helium loading to improve regeneration in the final two stages of the machine, and in the third example we introduced ^3He as the working fluid to further enhance the performance of the lowest temperature stage.

Although our calculations accounted for a substantial part of our total effort, we also addressed the more mechanical aspects of the cryocooler to the extent of developing a well defined approach which we feel is simple enough to have the requisite reliability yet elegant in concept. The basic premises which guided our mechanical design effort were as follows:

1. The magnetic, electrical, and vibrational signatures of the machine should allow the cryocooler to be used with very sensitive superconducting magnetic sensors.

2. An absolute minimum of moving parts in the engine will promote reliability and long life.

3. There should be no electrical power required at the cryocooler itself.

4. Moving seals should be required only to separate low pressure helium from high pressure helium, rather than helium gas from the open atmosphere.

5. The machine should operate at the lowest possible pressures to reduce forces (and wear) and to improve the reliability of the machine.

To a great extent we were able to achieve these goals in the mechanical design which we describe in Section III.

Since one of the applications of greatest interest here is using closed-cycle cryocoolers to cool superconducting magnetic sensors, our entire effort has been devoted to investigating the behavior of a device constructed entirely of magnetically clean materials. We have also given attention to the problem of eddy currents by using nonconducting materials where possible and keeping potential eddy current paths small where conducting materials are required. We have also included suggestions for coupling superconducting devices or electronics to the low-temperature end of the cooler, and for damping vibrations of the cryocooler. Although these two aspects of the design are subordinate to the initial task of obtaining sufficient refrigeration at the required temperature, both design elements will have to be rigorously solved before any cooling machine becomes a practical cryocooler.

Finally, we present a general description of the types of tests we intend to perform to measure the magnetic, electrical, and vibrational signatures of the device under its operating conditions. We intend to make the measurements using SQUID sensors and mutual inductance coils attached directly to the

cryocooler and its vacuum shield. This approach is particularly desirable since one of the important applications of cryocoolers operating below 10 Kelvin is the use of SQUID technology in magnetometry and gradiometry measurements.

II. STIRLING CRYOCOOLER DESIGN

In this section we discuss the major design elements of a cryocooler using a regenerative Stirling cycle. In keeping with our original proposal and motivated by the recent success of Zimmerman's Stirling cryocooler[1], we have selected the regenerative Stirling cycle for our proposed cryocooler, so our calculations for thermal losses in the machine are characteristic of the Stirling cycle. During the course of our work we considered the Stirling cycle as used in the Gifford-McMahon configuration where the pressure changes in the machine are obtained through the use of high and low pressure reservoirs and valves which alternately connect the engine to the two reservoirs. In the context of the design goals outlined in the last section, the Gifford-McMahon configuration has some distinct advantages.

A. General Design Considerations

To arrive at a "zeroth order" design for the cryocooler, we first considered various sources of thermal loss which must be balanced by the refrigeration capacity of the device. Because the cryocooler will operate over nearly three orders of magnitude in temperature, the thermodynamic properties of both the working fluid and the materials in the machine will change substantially so that different loss mechanisms will dominate in different parts of the machine.

During these preliminary studies we considered five mechanisms which clearly produce thermal loading of the cryocooler; regeneration loss, shuttle heat loss, conduction loss, viscous loss, and radiation loss. Each of these mechanisms will be described and quantitative estimates of their effects will be presented. We found that the most signficant of these mechanisms are regeneration loss in the coldest stages of the cryocooler, shuttle loss in the intermediate stages, and conduction loss in both the intermediate and warmest stages. With proper insulation the radiation losses appear to be almost negligible, and viscous losses are significant only in the warmest stage where the viscosity of the helium gas is relatively large and there is a high molar flow rate.

For our first estimates we considered a multistage Stirling device with a displacer consisting of concentric cylinders as shown schematically in Figure 1. In this type of cryocooler the refrigeration cycle consists of the following steps where step one begins with the displacer moved all the way toward the cold end of the machine and all of the working fluid is displaced to the warm end.

1. Compression of the fluid in the hot end to pressure P_{hi}
2. Regeneration of the fluid from the hot end to the cold end
3. Expansion of the fluid to pressure P_{lo}
4. Regeneration of the fluid from the cold end to the hot end.

For the geometry shown in Figure 1, the refrigeration occurs in the volumes labeled V_1 through V_4, and the regeneration occurs in the narrow annular gaps between the cylinder walls and the displacer. Except for the narrow regeneration gaps, the displacer fills the entire volume of the engine when it is moved toward the cold end, and the material in the displacer and cylinder walls provides the regeneration capacity of the device.

The refrigeration power at each stage in this design is given by:

$$\langle \dot{Q}_o \rangle = (T\beta)\, V_D\, \Delta P/\tau \qquad (1)$$

where T is the absolute temperature of the stage, β is the average isobaric expansion coefficient over the pressure range, V_D is the displaced volume of the stage, τ is the machine period, and ΔP is the pressure change during expansion. The refrigerating qualities of the working fluid are all contained in the quantity $T\beta$ (which is 1 for ideal gases), while V_D, ΔP, and τ are determined by the mechanical device itself. Consequently, by adjusting the mechanical parameters of the machine, we can adjust the refrigeration available at each stage. Since the thermal losses can also be expressed in terms of the working fluid parameters and the mechanical properties of the cryocooler, we can choose values which should provide sufficient refrigeration

Figure 1. General Geometry Of The Cryocooler

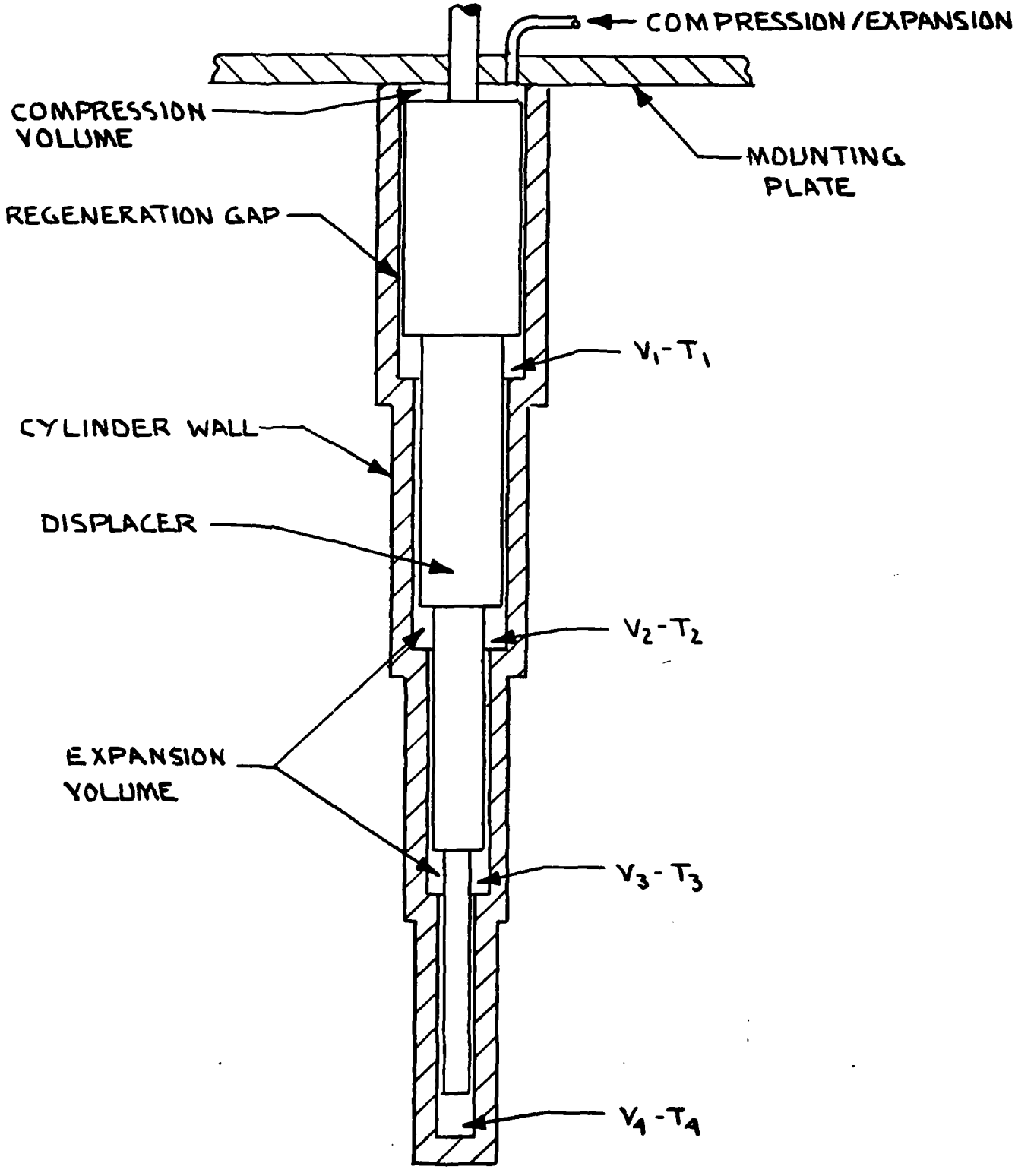

at each stage of the machine and yet be consistent with the design goals we outlined above. The parameters which are available for manipulation are:

1. The length and diameter of the displacer for each stage, L_i and D_i,
2. The regeneration gap for each stage, d_i
3. The displacer stroke, $2X_0$,
4. The high and low operating pressures, P_{hi} and P_{lo}, and
5. The engine cycle period, τ.

We approached the initial design by computing the expected losses for the coldest stage then selecting engine parameters for that stage which would provide the requisite refrigeration for the lowest temperature to be achieved. The displacer parameters and regeneration gap were then still available to optimize the performance of the higher stages. These calculations accounted for more than half of our total effort; a substantial part of this time was devoted to quantitatively describing the regenerative and shuttle losses to be expected in an engine of this type.

We applied our calculations to three different cases. We first considered a device in which both the displacer and cylinder walls consisted entirely of nylon, as in the machines built by Zimmerman. These calculations provided a basis from which we could compare our predictions with an actual experiment and, in addition, laid the foundation for later estimates which would include modifications to the regenerator and the use of ^3He as the working fluid.

B. Regeneration Loss

In a standard Stirling cycle, the displacer moves the working fluid back and forth between the hot and cold ends of the engine, and the refrigeration is accomplished by increasing the pressure of the fluid while it is in the hot end and decreasing the pressure while it is in the cold end. As the gas moves from the hot end of the refrigerator to the cold end, it will continuously cool by giving up heat to the relatively colder parts of the engine, and the process will be reversed when the gas moves in the other direction. This process is called regeneration, and in the geometry shown in Figure 1 the regenerator consists of the cylinder walls and displacer.

Ideally, when the fluid enters the cold end of the refrigerator it will already be at the ambient temperature, having been completely regenerated as it moved down the length of the machine. In fact, of course, the regeneration is not perfect, and the process will transport heat into the cold end. The resultant thermal loading is referred to as regeneration loss. Since virtually all of the fluid is warmed to room temperature during each cycle of the refrigerator, imperfect regeneration can produce tremendous thermal loading of the cryocooler. In our design regeneration loss becomes important at temperatures below about 50K, and below about 20K it completely dominates all other thermal loss mechanisms. In general, regeneration loss will limit the performance of all low-temperature regenerative cryocoolers.

1. Constant Pressure Vs. Constant Molar Volume Regeneration

In analyzing regeneration losses in a Stirling cycle cryocooler we encountered a fundamental effect which had a profound impact on our ultimate choice for a cryocooler design. To describe the effect we consider a simple single stage cooler using an ideal gas as the working fluid and operating betwen temperatures T_c and T_h with expansion occurring between pressures P_{hi} and P_{lo}. In Figure 2 we depict schematically two configurations. In Figure 2a the expansion is performed by the power piston, and regeneration occurs with a constant number of moles of working fluid in the engine. Let us refer to this as constant moles (CM) regeneration. In Figure 2b, pressure changes are accomplished by alternately connecting the engine to the high and low pressure reservoirs so that the regeneration is performed at constant pressure (CP). We first consider CM regeneration.

As the gas moves to the cold end of the engine, the pressure in the machine will drop by a factor of T_c/T_h according to the ideal gas law. Consequently, if the expansion process is to operate between pressures P_{hi} and P_{lo}, the initial pressure in the engine must be greater than P_{hi} by the factor T_h/T_c. For example, in a single stage cooler operating between 150K and 300K with a pressure change of 6 to 1 atmospheres (atm.) during expansion, the initial pressure in the machine would have to be 12 atm. The problem is substantially worse in a machine operating between 10K and 300K even using multiple stages

Figure 2. Regeneration At Constant Moles (CM)
And At Constant Pressure (CP)

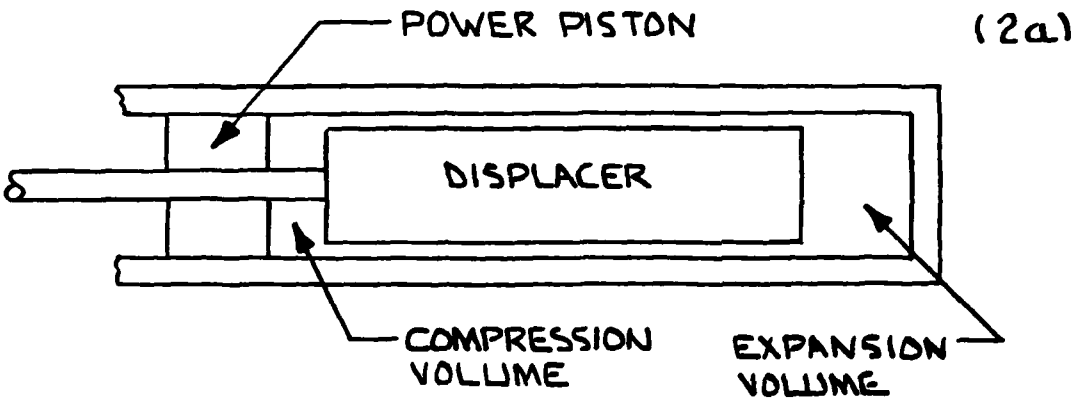

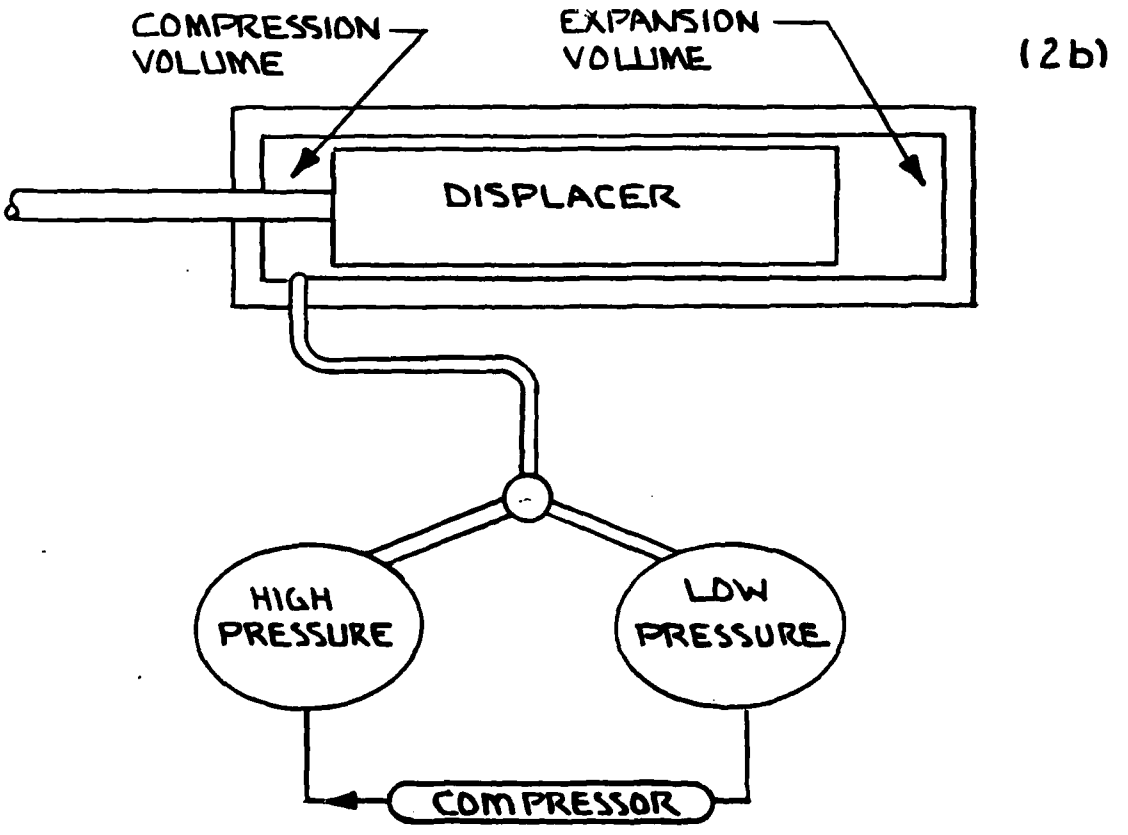

with decreasing volumes at the colder temperatures. For our tentative design (presented later in this section) CM regeneration would require that the hot-to-cold regeneration begin at a pressure of nearly 27 atm. However, in the interest of minimizing wear and enhancing the reliability of the cryocooler, one of our major design goals was to avoid pressures in excess of a few atmospheres.

Another disadvantage of CM regeneration concerns the rate at which the gas moves along the regenerator. In a simple single stage engine as in Figure 2a, when the displacer has moved through one-half of its stroke (equal volumes at hot and cold ends), most of the working fluid will already be residing in the cold end of the machine. Again using the ideal gas law, the ratio of the number of moles in the cold end to that in the hot end will be

$$n_h/n_c = T_c/T_h \qquad (2)$$

If the single stage is operating between 150K and 300K, then two thirds of the working fluid will be regenerated during the first half of the displacer stroke. As we show below, the regeneration loss is proportional to the square of the molar flow rate, hence the high flow rate during the first part of the regeneration process significantly enhances the regeneration loss. Again, the problem is substantially worse for a machine which operates over a temperature range of 10K to 300K.

In comparison, both of these problems are alleviated by using high and low pressures reservoirs to effect the pressure changes in the engine. (The technique of using external pressure reservoirs and valves is typically associated with the so-called Gifford-McMahon cycle.) In this mode, the regeneration occurs at constant pressure so that during hot-to-cold regeneration gas will flow into the engine from the high pressure reservoir and the flow rate of the fluid along the regenerator will be uniform during the regeneration. The major disadvantage of this configuration is that the use of pressure reservoirs results in an inherently lower cryocooler efficiency, since the expansion process allows the gas to expand into the low pressure reservoir where the expanding fluid performs no mechanical work which can be recovered by the system. Nonetheless, we feel that the advantages of

increased regeneration efficiency and the lower pressure requirements provide ample justification for an initial design using valves and pressure reservoirs to effect the pressure changes in the engine. In Appendix A we derive equations for the regeneration loss for both CM and CP regeneration which demonstrate the differences.

2. Model for Regeneration Loss

Since regeneration losses are the essential limitation in obtaining temperatures below 10K, we tried to analyze this particular problem in some detail. For a fixed cryocooler geometry the thermal conductivity and heat capacity of the working fluid and the regenerating material will determine the efficiency of the regeneration process. Specifically, the heat capacity and thermal conductivity of the working fluid determine respectively the amount of heat which must be regenerated, and the ease with which heat can move across the fluid from the center of the fluid gap to the wall where it can pass into the regenerator. Similarly, the thermal conductivity of the regenerator determines the rate at which thermal energy can diffuse into the regenerating material, and its heat capacity limits the total amount of heat which can be absorbed or given up during the regeneration process.

To model the regeneration loss, we first consider the case in which the walls allow perfect regeneration; that is the cylinder and displacer walls can absorb all of the heat of regeneration at constant temperature. If the fluid passes through the gap in a laminar flow (fluid velocity is maximum at the center of the gap and zero at the walls), the fluid in the center of the gap will be warmer than the fluid at the walls by an amount determined by the heat capacity, thermal conductivity, and the velocity of the fluid. In an annular gap of width, d, and diameter D, the heat flow along the gap produced by this effect is given by (see Appendix A):

$$\dot{Q}_r = \left(\frac{17}{140}\right)\left(\frac{d}{\pi D K_f}\right)\left(\dot{n}_o M C_p\right)^2 (\text{grad } T)_z \qquad (3)$$

where C_p, K_f, and M are respectively the heat capacity per unit mass (at constant pressure), the thermal conductivity, and the molecular weight of the working fluid, $(\text{grad } T)_z$ is the temperature gradient parallel to the flow direction, and n_o is the molar flow velocity along the regenerator.

To account for the heat capacity and thermal conductivity of the walls, we argue as follows. For a thermal wave of frequency ω in a medium of diffusivity κ, the wavelength of the thermal wave will be

$$\lambda = \sqrt{4\pi^2\kappa/\omega} = \sqrt{2\pi T\kappa} \tag{4}$$

where T is the period of oscillation. Hence, the effective penetration depth during one period of a thermal wave generated by an oscillating temperature at the boundary will be roughly one wavelength, and for a regeneration cycle, which takes approximately one quarter of the total engine period, τ, the effective thermal penetration depth, λ_d, will be approximately given by:

$$\lambda_d = \sqrt{\pi\tau\kappa/2} \tag{5}$$

In this picture, only that volume of regenerating material within about one penetration depth will contribute to the regeneration. Furthermore, we assume that during the regeneration process the temperature of this portion of the regenerator will increase or decrease approximately linearly in time, and that during the subsequent expansion or compression, the regenerator will relax back toward some equilibrium temperature due to diffusion within the regenerating material. We also assume that the displacer motion is linear during the regeneration process (as opposed to sinusoidal) and that the displacer is stationary during compression and expansion. For regeneration at constant pressure, the resulting regeneration loss is given by:

$$\langle \dot{Q}_r \rangle = .0608 \left(\frac{d}{\pi D K_f}\right)(C_p M \dot{n}_o)^2 (\text{grad } T)_z \left[1 + (.812)\left(\frac{K_f}{d}\right)\sqrt{\tau/K_w C_w}\right] \tag{6}$$

where K_w and C_w are respectively the thermal conductivity and heat capacity per unit volume of the walls, is the engine period, and C_p, K_f, M, D, d,

and $(\text{grad } T)_z$ are as defined in equation (3). The angular brackets around $\dot{Q}_R$ denote the time average over one engine cycle.

The first term in equation (6) represents the regeneration loss from thermal resistance across the fluid gap as in equation (3) while the second term gives the regeneration loss which results from the finite thermal conductivity and heat capacity of the walls of the regenerator. Note that the regeneration loss will increase rapidly as either the thermal conductivity or the heat capacity of the walls becomes small. Since nearly all materials display a very rapid decrease in both thermal conductivity and heat capacity near liquid helium temperture, this represents a fundamental problem for regenerative cycles at these low temperatures. In addition, the thermal conductivity of helium also decreases at low temperatures so that the thermal resistance across the fluid gap is also increasing.

3. Regeneration Loss In A Nylon Regenerator

To provide an illustrative comparison, we write equation (6) explicitly as two terms:

$$\langle \dot{Q}_r \rangle = \langle \dot{Q}_r \rangle_f + \langle \dot{Q}_r \rangle_w \tag{7}$$

where $\langle \dot{Q}_r \rangle_f$ represents the regeneration loss due to thermal resistance in the fluid itself, and $\langle \dot{Q}_r \rangle_w$ gives the loss due to the walls. These terms are defined by:

$$\langle \dot{Q}_r \rangle_f = (.0608)\left(\frac{d}{\pi DL}\right)(\dot{M}n_o)^2 \int_{\Delta T} (C_p^2/K_f)\, dT \tag{8}$$

and

$$\langle \dot{Q}_r \rangle_w = (.0494)\left(\frac{\sqrt{\tau}}{\pi DL}\right)(\dot{M}n_o)^2 \int_{\Delta T} (C_p^2/\sqrt{K_w C_w})\, dT \tag{9}$$

where now the integrals over the temperature range of regeneration, ΔT, account for the fact that C_p, K_f, C_w, and K_w all vary substantially as functions of temperature in the region of 10K. To provide the comparison we have evaluated equations (8) and (9) for the final stage of a cryocooler with the following parameters which are approximately those used by Zimmerman[1].

Regeneration gap:	$d = .0025$ cm
Displacer diameter:	$D = 0.47$ cm
Displacer length:	$L = 15$ cm
Displacer stroke:	$2X_o = 0.7$ cm
Engine period:	$\tau = 1$ sec
High pressure:	$P_{hi} = 8$ atm.
Low pressure:	$P_{lo} = 2$ atm

We have also assumed a constant temperature gradient, $\Delta T/L$ and that the final stage would operate with its high temperature end at 30K as indicated by the upper limit on the integrals. The heat capacity and thermal conductivity data for nylon were taken from Radebaugh and Zimmerman[2].

The results are plotted in Figure 3. The solid line shows the total refrigeration to be expected from equation (1) for this geometry; the broken line shows $\langle \dot{Q}_r \rangle_w$ for a stage in which both cylinder walls and displacer are made of nylon and ^{4}He is the working fluid. For comparison the dashed line shows the regeneration loss from the term $\langle \dot{Q}_r \rangle_f$. From Figure 3 it is clear that, for these engine parameters, a nylon regenerator produces an effective barrier at about 8 to 10 Kelvin where the regeneration loss will outstrip any possible improvement in refrigeration capacity.

We can also draw a comparison from Figure 3 between our computations and Zimmerman's experiments. Assuming that the wall-dominated regenerator losses completely dominate the thermal loss in this regime, we would estimate a low temperature limit for Zimmerman's machine of about 10.5 to 11 Kelvin, as determined by the intersection of the solid and broken lines in Figure 3. In fact, Zimmerman reports[1] that his device achieved a temperature of about 8.5 Kelvin. From his reported parameters, the available refrigeration curve in Figure 3 should be reasonably accurate, so the error probably lies in our estimates for the regeneration loss. Zimmerman's machine uses a sinusoidal cycle so our equation should probably contain an additional constant factor of order $\pi/4$. Also, instead of nylon, Zimmerman used G-10 fiberglass for his cylinder, but since the low temperature thermal conductivity and specific heat of G-10 are very similar to those of nylon, this should not represent a large

Figure 3. Refrigeration and Regeneration Loss Using An All Nylon Regenerator

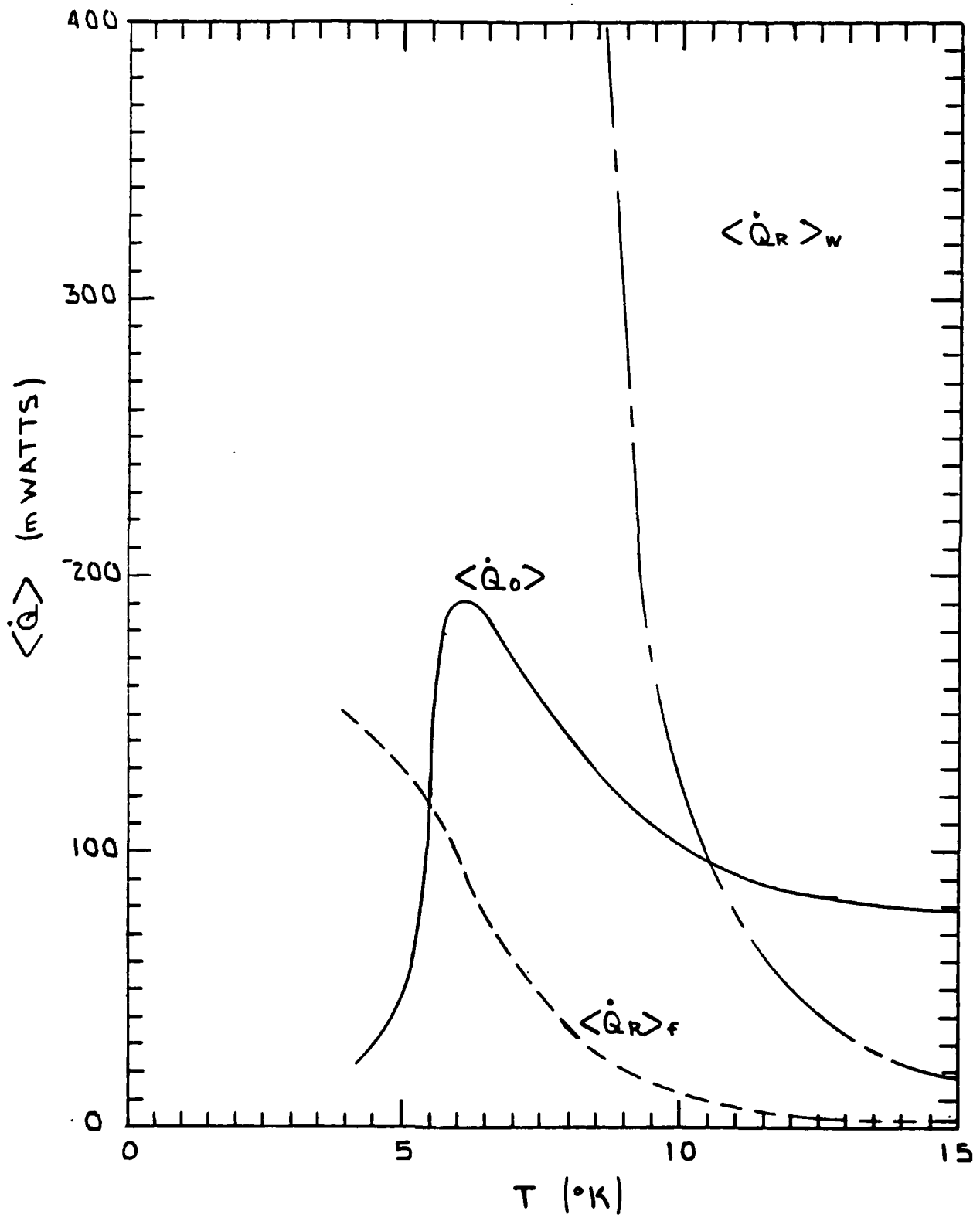

error. Even with these corrections it appears that we are overestimating the loss by roughly a factor of 2, so that our proposed design may allow for a greater regeneration loss than will actually be encountered. Nonetheless, since there may be effects for which we have not completely accounted, we have allowed for a regeneration loss as computed from equation (6) in our tentative cryocooler design.

The most straightforward approach to reducing the regeneration loss from the walls is to make the final stage longer since the loss is inversely proportional to the length through the factor $(\text{grad } T)_z$. But assuming reasonable lengths for an engine appropriate for field applications, the most optimistic estimates give only a factor of order 2 improvement, which would still result in an effective barrier in the region just below 10 Kelvin. Our approach to the problem is to change the thermodynamic characteristics of the walls in the regenerator passage in the coldest stage to provide more regeneration capability through increased heat capacity and improved thermal conductivity.

4. Regeneration Loss In A Helium-Loaded Regenerator

Figure 4 shows a schematic of our proposed technique for loading the walls of the lowest stage with helium. The static helium volume in the cylinder walls is connected to a room temperature helium reservoir which allows helium to continuously flow into the volume as the device cools down during start up. This eliminates the necessity for loading the regenerator with high pressure helium at room temperature to provide the necessary regenerative heat capacity at low temperature. The thermal connection between the heat capacity of the helium loaded regenerator and the helium working fluid will be provided by the laminated fiberglass-copper screen composite cylinder wall, in which the screens are spaced about one screen thickness apart. In this configuration, the copper screen will comprise about one-twelfth of the transverse area of the cylinder wall and about one-sixth of the total volume in the static volume. The resulting thermal conductivity of the cylinder wall, about one-twelfth that of solid copper, will then be sufficiently large that it will not contribute to the regeneration loss; that is, the regeneration loss in the

Figure 4. Helium Loading To Improve Low Temperature Regeneration

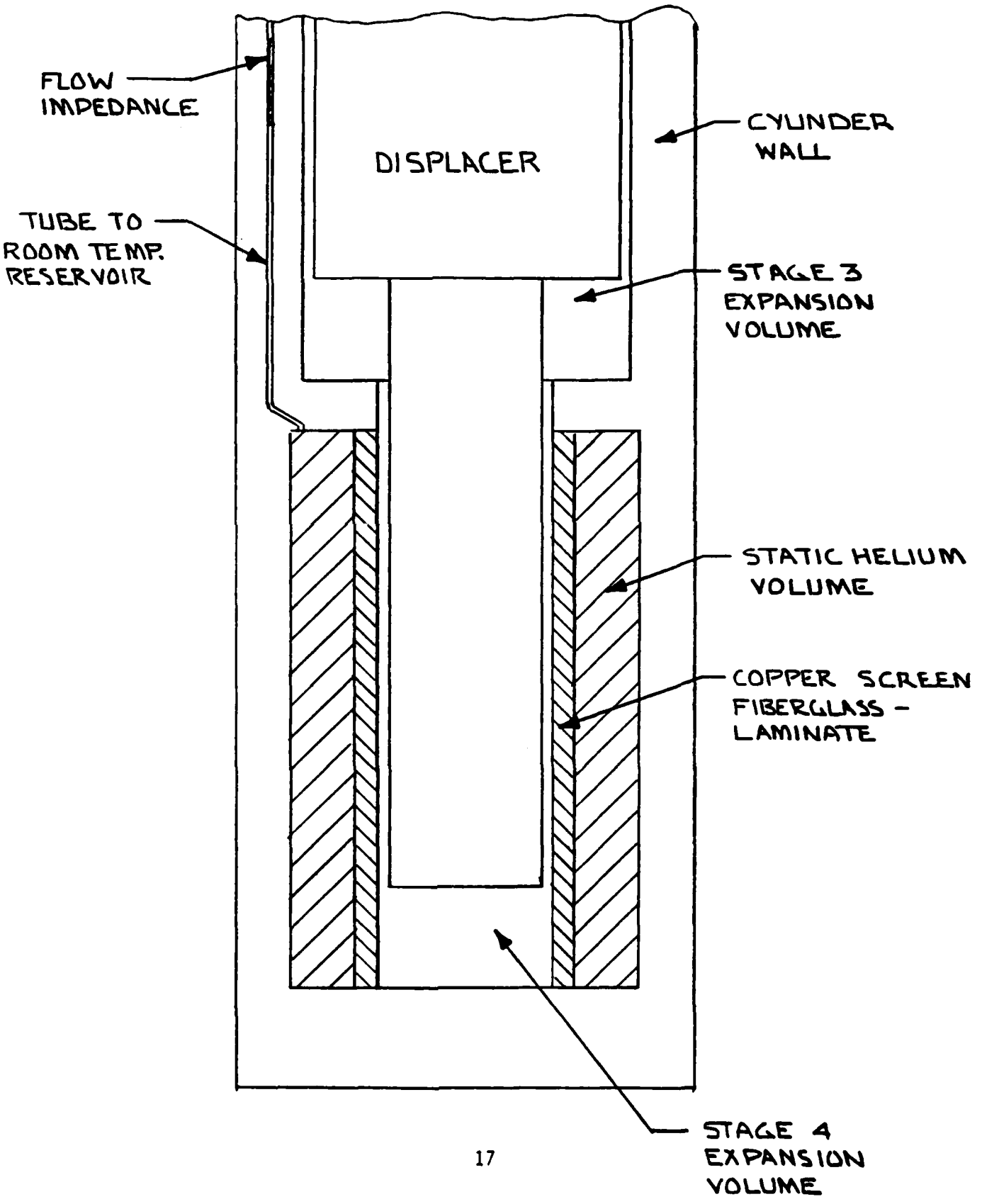

walls will arise only from the available heat capacity in the static helium. Also, all of the helium will be in good thermal contact with the copper screen since the penetration depth in helium at 10K is about 0.1 cm.

We can now estimate the regeneration loss for this geometry assuming that the heat capacity of the regenerator resides in the helium and the thermal conductivity of the wall is given by the copper, and we find:

$$\langle \dot{Q}_r \rangle = (.186)\left(\frac{d}{\pi D K_f}\right)(C_p \dot{M} n_o)^2 (\text{grad } T)_z \left\{1 + (1.346)\frac{K_f D \tau}{d(\rho C_p)_s (D_2^2 - D_1^2)}\right\} \quad (10)$$

where $(\rho C_p)_s$ in the second term is the heat capacity per unit volume of the static helium, and D_1 and D_2 are respectively the inner and outer diameters of the static helium volume. Note that the thermal conductivity of the copper screen does not enter into this expression, and that the constant factor in front of the first term is different from that in equation (6) as a result of the regeneration being limited to only one surface of the annular regeneration gap (see Appendix A).

For the data shown in Figure 5, we used the engine parameters which are typical of our tentative engine design (described later in this section) and which, for the coldest stage are:

Regeneration gap	$d = .005$ cm
Displacer diameter	$D = 1.0$ cm
Displacer length	$L = 15.0$ cm
Displacer stroke	$2X_o = 0.7$ cm
Engine period	$\tau = 3$ sec
High pressure	$P_{hi} = 6$ atm
Low pressure	$P_{lo} = 2.5$ atm

where P_{lo} was taken to be 2.5 atm to avoid operating below the critical pressure of ^{4}He. We also used 2.5 cm and 2.0 cm for the outer and inner diameters of the static helium volume. For these parameters the second term in equation (10) is negligible so the regeneration loss is determined by the characteristics of the fluid gap.

Figure 5. Refrigeration and Regeneration Loss In A Helium Loaded Regenerator With ^4He As The Working Fluid

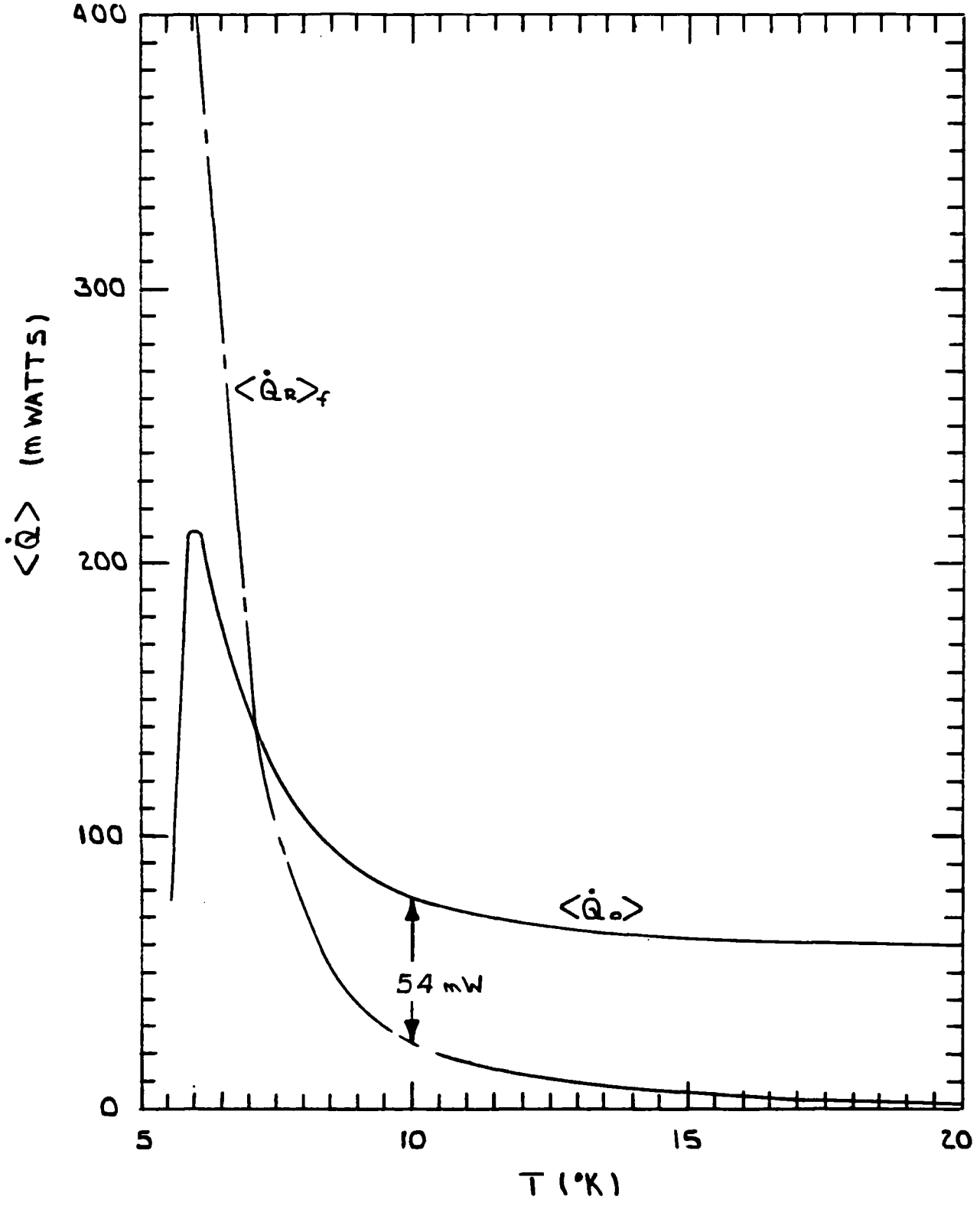

Since the contribution from the regenerator is completely negligible for this geometry, in Figure 5 we have plotted only the regeneration loss from the fluid gap and the expected refrigeration for the above parameters. It is interesting to note that even though the regeneration losses from the walls have been suppressed, there are still substantial losses in the fluid gap itself due to the increasing density and decreasing thermal conductivity of the helium. The effect is enhanced by the fact that regeneration can occur at only one of the surfaces in the regeneration passage, and, compared to our analysis for Zimmerman's machine, we are using a regeneration gap of .005 cm instead of .0025 cm. In fact, we could probably use a somewhat smaller gap in an actual machine, but based on our investigation of viscous losses (subsection E below), we can show that decreasing the gap below .005 cm begins to introduce viscous losses large enough to load the refrigeration capability of the coldest stage of the machine.

From Figure 5 it is clear that, if our assumptions and calculations are valid, the regeneration loss in our design will be limited by the fluid gap and not by regeneration losses in the walls. Another interesting observation is that below about 6K the refrigeration capacity of ^{4}He drops precipitously due to the temperature dependence of $T\beta$, so that even if the regeneration losses could be suppressed, the low temperature limit of the machine will still be about 6K. Nonetheless, for a cryocooler to have wide applicability for cooling a variety of superconducting instrumentation, we feel that it is desirable to achieve the lowest possible temperature.

5. Regeneration Loss Using ^{3}He

One method of further suppressing the regeneration loss and simultaneously obtaining refrigeration at a lower temperature is to substitute ^{3}He as the working fluid in the device. The primary advantage realized here is that both the critical temperature and critical pressure of ^{3}He are substantially lower than those of ^{4}He (3.3K and 1.2 atm for ^{3}He compared to 5.2K and 2.26 atm for ^{4}He). Consequently, the rapid increase in the density of ^{3}He as it aproaches its critical temperature occurs at a lower temperature and the result is directly reflected in the regeneration loss. In Figure 6 we show

Figure 6. Refrigeration and Regeneration Loss In a Helium Loaded Regenerator With ^3He As The Working Fluid

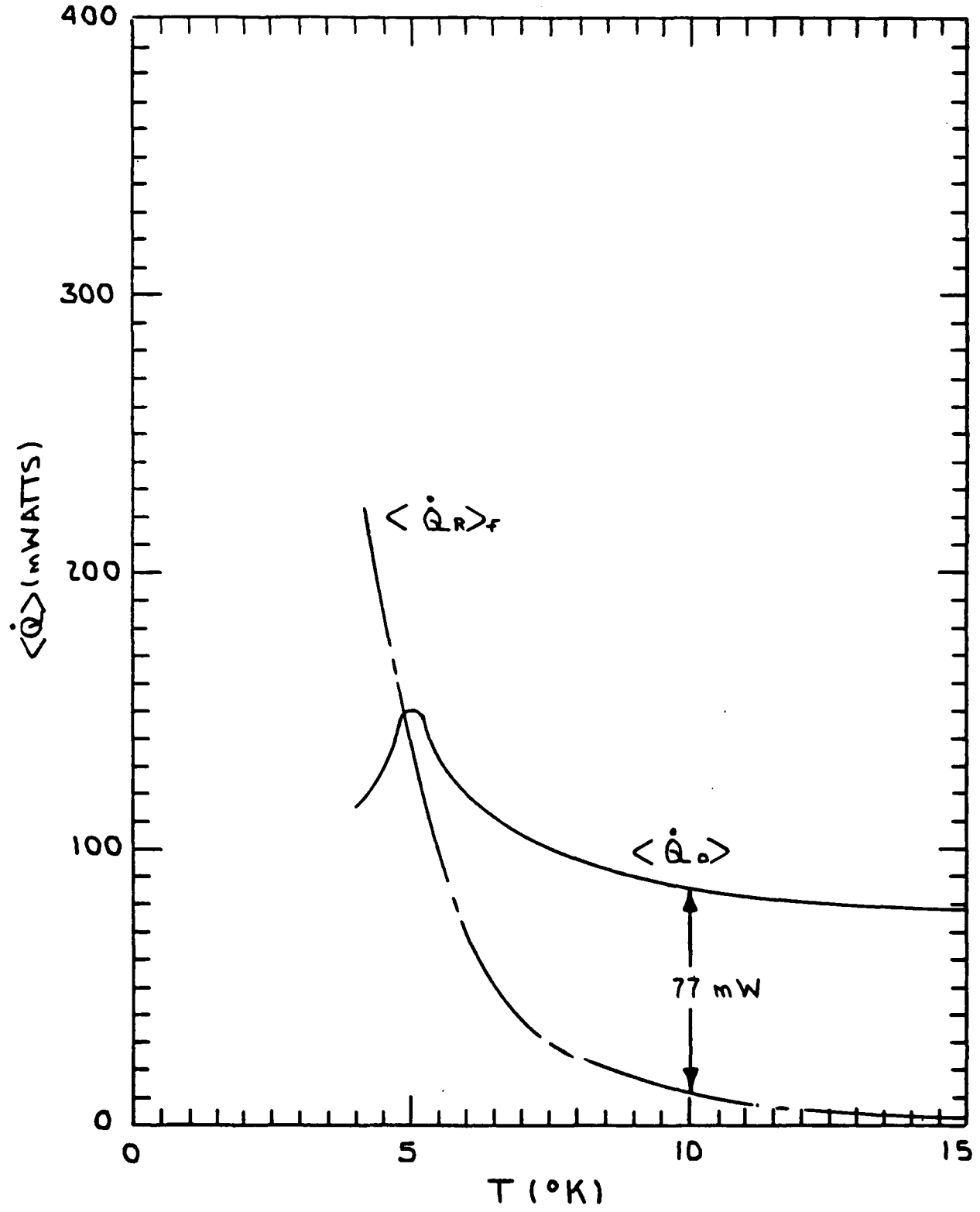

the regeneration loss for ^3He for the same parameters as the ^4He data in Figure 5 with the single exception that P_{lo} is taken as 1.3 atm for the ^3He data. As with the ^4He data, the contribution from the walls is negligible when compared to the loss from the fluid gap.

In comparing Figures 5 and 6 we note that the total refrigeration available when using ^3He is actually less than from the ^4He but the maximum refrigeration of about 150 mwatts is available at a lower temperature. In addition, the regeneration losses for ^3He become prohibitive at about 4 to 5 Kelvin compared to a range of about 6 to 7 Kelvin for ^4He. Both of these effects can be attributed to the lower critical temperature and pressure of ^3He.

The data for ^3He between 4 and 10 Kelvin presented a somewhat unique problem in that few measurements of the thermodynamic properties of the fluid have been performed in this temperature range. To make our comparisons we estimated the values for the density, specific heat, and refrigeration parameter, $T\beta$, by using data for ^4He and the law of corresponding states. In brief, the law of corresponding states assumes that the equations of state for ^3He and ^4He will be identical when expressed in a reduced (dimensionless) form in which the pressure, temperature, and volume are divided by their values at the critical point. For example, graphs of density versus temperature for ^3He and ^4He should be identical if plotted in the dimensionless form of ρ/ρ_c versus T/T_c. This approach will certainly fail at temperatures where Fermi and Bose statistics become important (at about 2 - 3 Kelvin for ^4He), but over the temperature range of interest to us both fluids are still above their critical temperature and their behavior is more gas-like than liquid-like. Hence for our estimates the approximations should be more than adequate. Data for the viscosity and thermal conductivity of ^3He were taken from the calculations of Monchick, et. al[3].

To summarize from Figure 5 it appears that with the proper regenerator design, a machine might be constructed which could reach about 6K using ^4He as the working fluid. This observation is even more encouraging when we recall that, based on a comparison with Zimmerman's experiments, we may be overestimating the regeneration losses. In addition, our calculations for ^3He have verified our original idea for achieving temperatures of 4 to 5 Kelvin by using ^3He as

the working fluid. From the estimates in Figures 5 and 6 it also appears that there should be at least 50 mwatts of refrigeration at 10K available to cool superconducting instrumentation attached to outside of the cryocooler.

6. Regenerator Heat of Expansion and Compression

There is one final aspect of the regenerator which we have also considered. In an idealized engine the regenerator is typically assumed to have zero volume, and for most of our calculations this was a reasonable assumption. However any practical regenerator will have a finite volume which leads to the following effect. During the expansion process the fluid in the regenerator will cool and absorb heat from the regenerator walls; similarly, during compression the fluid will tend to give heat up to the regenerator. The net result of the effect is to increase the thermal loading on the regenerator. If the regenerator does not have sufficient heat capacity to provide the requisite heat of expansion and comopression to the fluid, the final result will be a net transport of heat down the cryocooler.

We have examined the magnitude of the problem in our tentative design and find that, for our regenerator geometry, the heat of expansion and compression in the coldest stages of the cryocooler will be about ten percent of the total heat of regeneration. In the warmer stages of the machine the percentage effect is less, which is consistent with our observation that the regeneration loss is small above about 50K.

While a ten percent effect is certainly not negligible, our calculations are probably not sufficiently precise to fully account for effects which enter at this level. Nonetheless, we now know the expected magnitude of the mechanism, and during the development program we will perform measurements designed to investigate it.

C. Conduction Losses

Conduction loss in the engine is easily found by estimating the amount of heat which flows along the displacer and the cylinder walls due to the temperature gradient along the axis of the machine. In analyzing the performance of a

given design we computed the conduction loss only for heat flowing downward from the next warmer stage; that is, we have assumed that all the heat flowing down the displacer and cylinder walls of a particular stage is effectively removed at the next cooling stage. The conduction loss for each cooling stage of the engine, $\langle \dot{Q}_c \rangle$, is then just:

$$\langle \dot{Q}_c \rangle = K\left(\frac{A}{L}\right) \Delta T \qquad (11)$$

where A is the cross-sectional area of the stage, L is the length, K is the average thermal conductivity of the material comprising the stage, and ΔT is the temperature difference between this stage and the next higher stage. In the coldest parts of the machine the conduction loss in the nylon displacer and cylinder walls becomes negligible due to the decreasing thermal conductivity of the nylon; however, conduction losses in the higher stages of the machine place a significant limitation on the design parameters of the first two stages.

In particular, as the displacer and cylinder increase in diameter to accommodate the intermediate cooling stages, thermal conduction along the axis of the machine increases in direct proportion to its cross-sectional area. Furthermore, in the warmer stages of the machine where the cross-sectional area is large, the thermal conductivity of the nylon is also increasing.

Unfortunately, the only simple solution to this problem is to reduce the A/L ratio by increasing the length of the machine which is inconsistent with our desire to keep the device small and compact. In principle, one could build a hollow displacer for the warmer parts of the machine and either evacuate the resulting volume or fill it with a heavy gas such as nitrogen which has a thermal conductivity roughly an order of magnitude less than that of nylon. The difficulty arises when the helium working fluid is introduced into the machine because helium gas readily diffuses through virtually all plastics at room temperature. Since the thermal conductivity of helium is nearly as large as that of nylon, any improvement in conduction loss realized by using a hollow nylon displacer would be lost soon after start up.

One configuration in which this approach might be used is in the construction of a welded thin-walled metal displacer. The use of a magnetically clean, high-resistivity metal would help suppress the magnetic and eddy current signatures but for the particular application being considered here this approach would probably not be desirable. In any event, we have arrived at a design which should provide sufficient cooling power at the intermediate stages of the machine to compensate the expected conduction losses.

D. Shuttle Heat Loss

The next thermal loss mechanism we examined was shuttle heat loss which arises from the shuttling motion of the displacer between the hot and cold ends of the engine. Thermal loss occurs in the engine because the displacer absorbs heat while it is toward the warm end of the machine, and heat will flow out of the displacer into the cylinder walls when the displacer is toward the cold end of the machine. For example, at the end of the cold-to-hot regeneration process the displacer will be toward the warm end of the machine so that at each point along the machine the walls of the displacer will be slightly cooler than the cylinder wall. Consequently while the displacer is stationary during the ensuing compression, heat will flow across the gap tending to equalize the temperature of the displacer and cylinder walls. When the displacer moves toward the cold end of the cryocooler, the process is reversed resulting in a transfer of heat toward the cold end of the machine.

As with the regeneration loss, we assumed an articulated engine cycle in which the displacer is stationary at its extreme positions during the compression and expansion portions of the engine cycle, and that only an effective thermal skin depth in both the walls and displacer participates in the mechanism. The equation which describes the process is (see Appendix B):

$$\langle \dot{Q}_s \rangle = (\pi D X_o^2) \sqrt{2\pi K_d C_d / \tau} \; (\text{grad } T)_z \; (1 - e^{-\alpha\tau/2}) \qquad (12)$$

where D is the displacer diameter and $2X_o$ is its stroke, τ is the engine period, C_d and K_d are respectively the specific heat per unit volume and

thermal conductivity of the displacer, and α^{-1} represents an effective time constant where:

$$\alpha = (K_f/d)\sqrt{2/\pi K_d C_d \tau} \qquad (13)$$

As before, d is the regenerator gap, and K_f is the thermal conductivity of the working fluid.

The shuttle heat loss increases with increasing displacer stroke and decreases as the engine period increases as one would expect. It is also interesting to note that when the heat capacity and thermal conductivity of the displacer are large (small α) the shuttle heat loss has the form

$$\langle \dot{Q}_s \rangle \simeq \left(\frac{\pi D K_f}{d}\right) X_o^2 \, (\text{grad } T)_z, \qquad \alpha\tau << 1 \qquad (14)$$

in which the loss is determined by the thermal conductivity of the working fluid and the size of the gap. In the other extreme, where α is large, the equation takes the form:

$$\langle \dot{Q}_s \rangle \simeq (\pi D X_o^2)\sqrt{2\pi K_d C_d/\tau} \, (\text{grad } T)_z, \qquad \alpha\tau >> 1 \qquad (15)$$

in which the loss is determined by the thermal conductivity and heat capacity of the displacer. As with conduction losses, shuttle heat losses are negligible in the lowest temperature stages but impact on design parameters of the warmer stages.

It is of interest to compare the results in equations (14) and (15) with Radebaugh's calculations for sinusoidal motion[2,4]. Radebaugh's equations would predict that the term in equation (14) would be reduced by a factor of 2, while the expression in equation (15) should be a factor of $\sqrt{8}$ smaller. The magnitude of the discrepancy is somewhat disturbing since we expect factors of only order $\pi/4$ to represent the difference between articulated and sinusoidal motion. Also Radebaugh has compared his calculations with his measurements of shuttle heat and found good agreement at temperatures above 100 Kelvin. If we are indeed overestimating the shuttle heat losses in our device, the problem may lie in considering only one skin depth in the dis-

placer and walls. Nonetheless, for our purposes here we will continue to use our own estimates since any overestimation of thermal loss represents a more strigent requirement on our design which can perhaps be relaxed at a later date.

E. Viscous Losses

Viscous losses in the cryocooler will tend to generate heat in the working fluid as it is cycled back and forth through the regenerator passages. We derive the expression for the viscous loss in Appendix C; here we quote only the result. For the final stage of the cryocooler, the viscous loss is given by:

$$\langle \dot{Q}_v \rangle = 48\pi \left(\frac{D}{d}\right)^3 \left(\frac{X_o \rho_o}{\tau}\right)^2 \left[(\text{grad } T)_z\right]^{-1} \int_{\Delta T} \frac{\eta}{\rho^2} dT \qquad (16)$$

where ρ_o is the density of the fluid at the bottom of the last stage, η is the temperature dependent viscosity, and ρ is the temperature dependent density of the fluid in the regenerator. For the higher stages where the helium is essentially an ideal gas, equation (16) becomes:

$$\langle \dot{Q}_v \rangle = 12\left(\frac{R\dot{n}}{P}\right)^2 \left[\pi D d^3 (\text{grad } T)_z\right]^{-1} \int_{\Delta T} \eta T^2 dT \qquad (17)$$

where P is the pressure of the gas, R is the gas constant, and $\dot{n}$ is the molar flow rate through the regenerator.

For our typical engine parameters, the viscous losses become significant only in the warmest stage Note however that the viscous loss is proportional to d^{-3} so that a small increase in the regenerator gap in the first stage (and perhaps also the second) will reduce the effect to a secondary level. Since the regeneration loss in these stages is small, the increased regeneration gap will not adversely affect the performance of the warmer stages.

F. Radiation Loss

Finally, heat will leak into the low temperature parts of the cryocooler through thermal radiation from the room temperature vacuum container which

will surround the cryocooler. We expect to solve this problem in a manner analogous to that used in insulating liquid helium dewars. Each stage of the machine will be surrounded with multiple layers of superinsulation, and a thermal shield which will be thermally grounded to the high temperature end of the stage. Since the thermal shields will be attached to the cryocooler at exactly the points where refrigeration is readily available, nearly all of the thermal energy radiated into the superinsulation should be removed at the intermediate stages of the machine.

The most significant load from thermal radiation should fall on the first stage and our estimated value for the radiation loss at this point is of order 140 mWatts. While this value is not insignificant, it certainly does not represent the limiting factor in the performance of the first stage of the cryocooler. Similarly, the radiation losses at the colder stages are small compared to other losses we have discussed. For example, the anticipated radiation loss at the cold end of the machine should of order 0.2 mWatts.

G. Summary of Cryocooler Design

In the preceeding paragraphs we have outlined our approach to analyzing the performance of a Stirling cycle cryocooler and discussed the principal elements of the thermal losses we expect and the impact of each mechanism on a tentative design. In Table 1 we show the estimated losses from all of the above sources at each stage in the machine. The column labelled $\langle \dot{Q}_o \rangle$ gives the estimated refrigeration available at each stage from equation (1) and $\langle \dot{Q}_{ext} \rangle$ gives the residual refrigeration which should be available as external refrigeration for cooling electrical leads or other apparatus external to the cryocooler. These data clarify our earlier discussions regarding the roles of regenerative, shuttle, and conductive heat losses at different stages of the machine. It is clear that while shuttle and conduction losses do not play a significant role in the coldest stage of the machine, in the two warmest stages both effects have a substantial impact on the performance of the machine. In stage two we note that the estimated losses consume nearly the entire refrigeration capacity of the stage leaving very little refrigeration available for external cooling. However, since regeneration loss, shuttle loss, and conduction loss are all inversely

Table 1. Zero Order Engine Parameters

Stage	T (°K)	D (cm)	d (cm)	L (cm)	$\langle\dot{Q}_o\rangle$ (mw)	$\langle\dot{Q}_R\rangle$ (mw)	$\langle\dot{Q}_s\rangle$ (mw)	$\langle\dot{Q}_c\rangle$ (mw)	$\langle\dot{Q}_v\rangle$ (mw)	$\langle\dot{Q}_{rad}\rangle$ (mw)	$\langle\dot{Q}_{ext}\rangle$ (mw)
1	175	5	.015	15	3004	113	854	827	164	140	906
2	75	3.5	.015	20	648	91	251	252	20	3.9	34
3	30	2	.010	15	235	66	52	42	7.5	1.8	67
4	10	1	.005	15	86	11	4.5	7.2	13	---	50

D = Displacer diameter
d = Regenerator gap
L = Regenerator length
$\langle\dot{Q}_o\rangle$ = Refrigeration power
$\langle\dot{Q}_R\rangle$ = Regenerator loss
$\langle\dot{Q}_s\rangle$ = Shuttle loss
$\langle\dot{Q}_c\rangle$ = Conduction loss
$\langle\dot{Q}_v\rangle$ = Viscous loss
$\langle\dot{Q}_{rad}\rangle$ = Radiation loss
$\langle\dot{Q}_{ext}\rangle$ = External refrigeration

Displacer Stroke: $2X_o$ = 0.6 cm
High Pressure: P_{hi} = 6.0 atm
Low Pressure: P_{lo} = 1.0 atm
Engine Period: τ = 3 seconds

proportional to the length of the stage through the (grad T)$_z$ factor, we can improve the situation by making the second stage longer. For example, the external refrigeration at stage two could be increased to 143 mwatts at the expense of lengthening the second stage regenerator to 25 cm.

With regard to Table 1, we wish to emphasize here that our work thus far has been purely exploratory and the cryocooler parameters presented do not represent a firm design for hardware construction. Rather, these data are intended only as a guide to further investigations which we feel should begin by attempting to understand the role of each of the thermal loss effects in a real device. Specifically we intend to begin the hardware development program by constructing a simple single stage-device suitably instrumented for performing measurements of various thermal losses which can be compared to our predictions. Direct comparison of experimental measurement with calculated predictions can then lead to refinements in our picture of the operation of the cryocooler and a more definitive design for multistage machines.

There is an interesting point to be made here concerning trade-offs between different parameters in the machine and our procedure for selecting those values given in Table 1. In making our initial guesses for the engine parameters we first considered the coldest stage and selected a set of parameters which would provide sufficient refrigeration at 10K to compensate the expected losses and still provide the requisite external refrigeration. For example, we initially chose the pressure change during expansion to be 3 atmospheres instead of 5. Although there is much less refrigeration available from the smaller pressure change, the regeneration loss in the coldest stage also decreases with pressure. Unfortunately however, the dominant thermal losses in the warmer stages are shuttle and conduction loss which are independent of the engine operating pressure, and as one increases the displacer diameter to provide more refrigeration the conduction loss increases at nearly the same rate. Consequently, the larger pressure change is required to provide adequate refrigeration in the warmest stages of the machine.

In a larger view, the entire engine design must be balanced through a system of trade-offs such as using longer engine periods and low pressures to promote reliability at the expense of less cooling power and longer cool down times,

or using a longer engine design to decrease thermal losses at the risk of incurring more serious vibrational problems. Since there are a variety of design parameters which can be manipulated in this fashion, optimizing the final device will require that we gain a firm understanding of the device through a well-organized, systematic approach to the basic principles involved.

To summarize, Table 1 represents a first attempt to optimize a Stirling cycle cooler by balancing estimated losses against available refrigeration with consideration given to the requirements for external refrigeration and to the design goals we outlined in the Introduction. These estimates will provide guidance in constructing our first simple machine, but during the early part of the development program it will be essential to refine, and modify if necessary, our present theoretical description. Once we have a firm understanding of the behavior of a simple machine, we can modify the estimates in Table 1 as required and proceed to a more complex machine.

III. MECHANICAL DESIGN OF THE CRYOCOOLER

In the mechanical design of the cryocooler we include the details of the construction of the cylinder and displacer, the mechanism for driving the displacer, the means for providing pressure changes in the device, and, in the event we use pressure reservoirs, the means for compressing the helium and the valves by which the device is alternately connected to the high and low pressure reservoirs. These aspects of the design are extremely important in the context of the design goals listed in the Introduction, for example, the use of sliding seals, the power requirements, and thermal coupling to the cryocooler.

A. Motive Power

Two processes in the cryocooler require some source of motive power; namely the compression and expansion processes and the displacer motion. In view of the stringent requirements on the magnetic and electrical cleanliness of the cryocooler, we have not seriously considered the possibility of using electrical devices at the cryostat head to provide the displacer motion, especially any type of solenoid valves or motors which might contain high permeability materials. The alternative which we favor is fluid pressure in the form of either a pneumatic or hydraulic system. The major advantage of a fluid system is that the fluid compressor and its motor drive can be located remotely and connected to the cryocooler via flexible lines in a split Stirling type of arrangement. This configuration greatly eases the electrical and magnetic requirements on the fluid compressor, and isolates the cryocooler from compressor vibrations. An additional feature of using a fluid displacer drive is the possibility of integrating the displacer drive with the high and low pressure helium reservoirs in a Gifford-McMahon type of engine configuration. The pressure difference between the two helium reservoirs then provides the energy for moving the displacer at the cost of a slightly higher throughput at the compressor.

The other requirement on a power source for the cryocooler is for compression and expansion of the working fluid for which there are essentially two

options: either physically changing the volume of the engine, or causing gas to flow into or out of the engine during the compression and expansion processes. For our estimated operating pressure range of 1 to 6 atmospheres, the engine volume at the warm end would have to change by a factor of 6 to produce the required compression.

At one atmosphere the total volume of the engine will have to be of order 300 cm^3 to accommodate our estimated molar volume at low temperature, so that the volume of the engine will have to change by about 250 cm^3 during the compression process. Volume changes of this magnitude (with the resulting pressure changes) would almost certainly require a piston type of compression arrangement, rather than a bellows or a rolling seal, with the complication of the added piston seals. It is also vital that all seals between the helium and the atmosphere be absolutely leak tight to prevent air from getting into the cryocooler and solidifying in the regeneration passages.

In Figure 7 we show a schematic of our concept of a simple system which provides for the motive power requirements at the cryocooler head and fulfills most of the design goals outlined previously. In this configuration the two helium reservoirs are located at the cryostat head with the entire mechanical system and the high pressure reservoir (exclusive of the compressor) contained within the low pressure helium reservoir. The only connections between the cryostat and outside world are the high pressure helium line from the compressor and the helium return line. The helium compressor is located remotely to avoid electrical interference from the compressor drive.

The interesting features of the design are as follows:

1. There are no dynamic seals between the helium working fluid and the atmosphere (with the possible exception of the compressor).

2. The only dynamic seals will be in the pneumatic valves and around the displacer and these seals will separate only low pressure and high pressure helium.

Figure 7. Schematic For Mechanical Arrangement For Displacer Drive and Compression/Expansion Processes

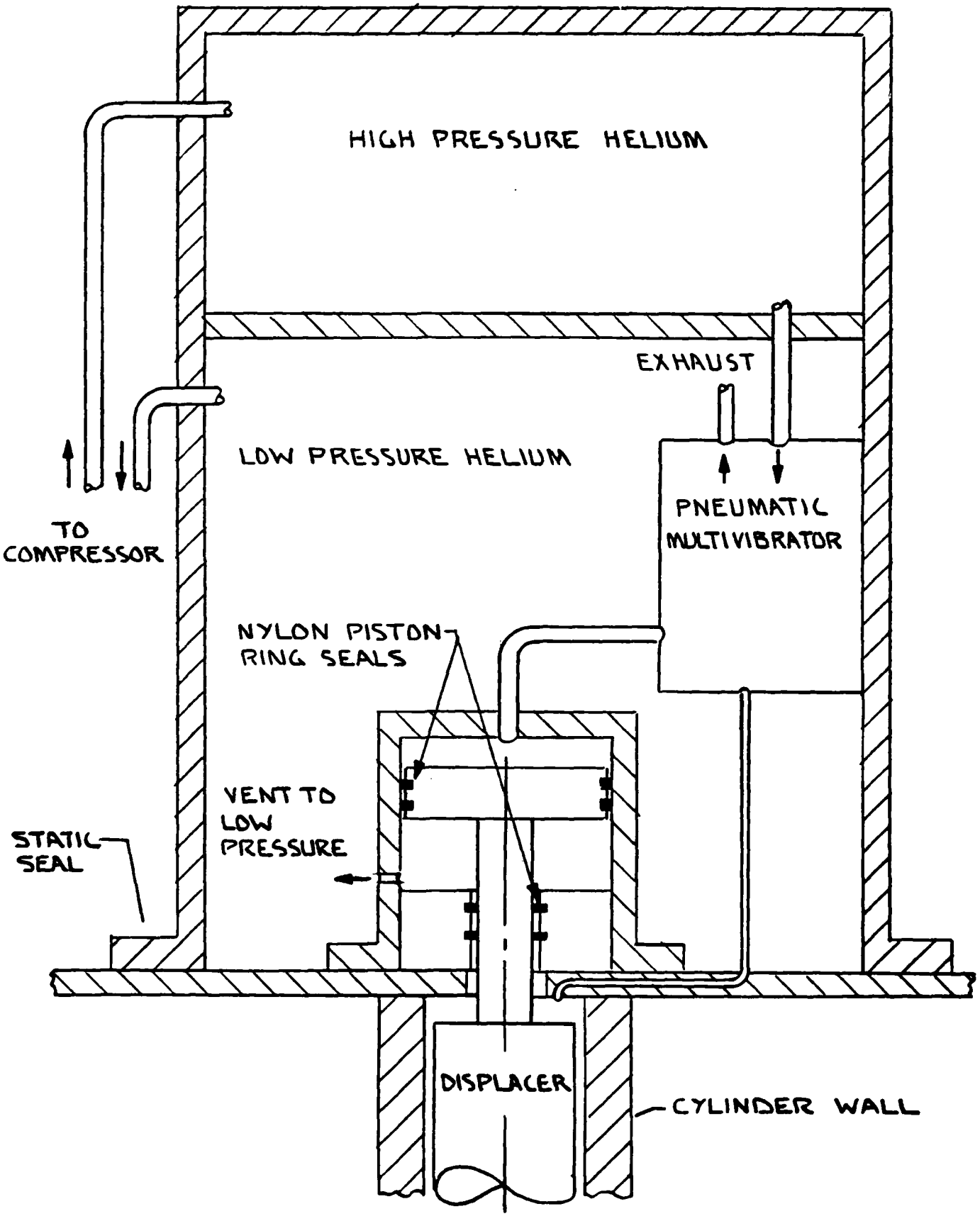

3. The only input to the cryostat is the unidirectional flow of helium gas to maintain the reservoir pressure differential.

4. The displacer motion and compression/expansion processes are actuated by a "pneumatic multivibrator" which is self-starting and provides the correct displacer phasing with respect to the pressure changes.

This last item requires further explanation. A common component in pneumatic systems is the pneumatic spool valve which is operated with a pneumatic pilot signal. In Figure 8 we show a schematic of an appropriate penumatic multivibrator in which the components labelled with Z's represent pneumatic flow impedances and the pneumatic spool valves (SV1 and SV2) control the pressure in the engine and the displacer motion through impedances Z_p and Z_d respectively. The impedances Z_1 and Z_2 with their respective dead volumes V_1 and V_2 provide the proper timing for piloting the spool valves. The spool valves are extremely simple in construction and can easily be constructed from magnetically clean materials if nonmagnetic versions are not available commercially. The table in Figure 8 shows the four steps in the engine cycle with the corresponding positions of the two spool valves for each of the four processes which comprise the total cryocooler cycle.

Although this is our preferred design due to its simplicity, we recognize that pneumatic systems are inherently "soft" (highly compressible) and that the pneumatic displacer drive may not provide a sufficiently uniform motion for the displacer stroke. An alternative technique is to drive the displacer using an incompressible hydraulic fluid but if this technique is adopted it will necessitate a completely leak proof seal between the hydraulic fluid drive and the helium in the engine. Since the displacer stroke is only 0.6 cm a bellows seal could possibly be used but the pressure of 5 atmospheres across the bellows would probably shorten its usuable lifetime substantially.

B. Power Requirements

It is a little difficult to set a firm value on the total power requirements of the cryocooler as we do not yet have a feeling for what the mechanical losses in the system will be. However, we can make some estimates concerning

Figure 8. Pneumatic Multivibrator For Displacer Drive and Generating Expansion/Compression Processes

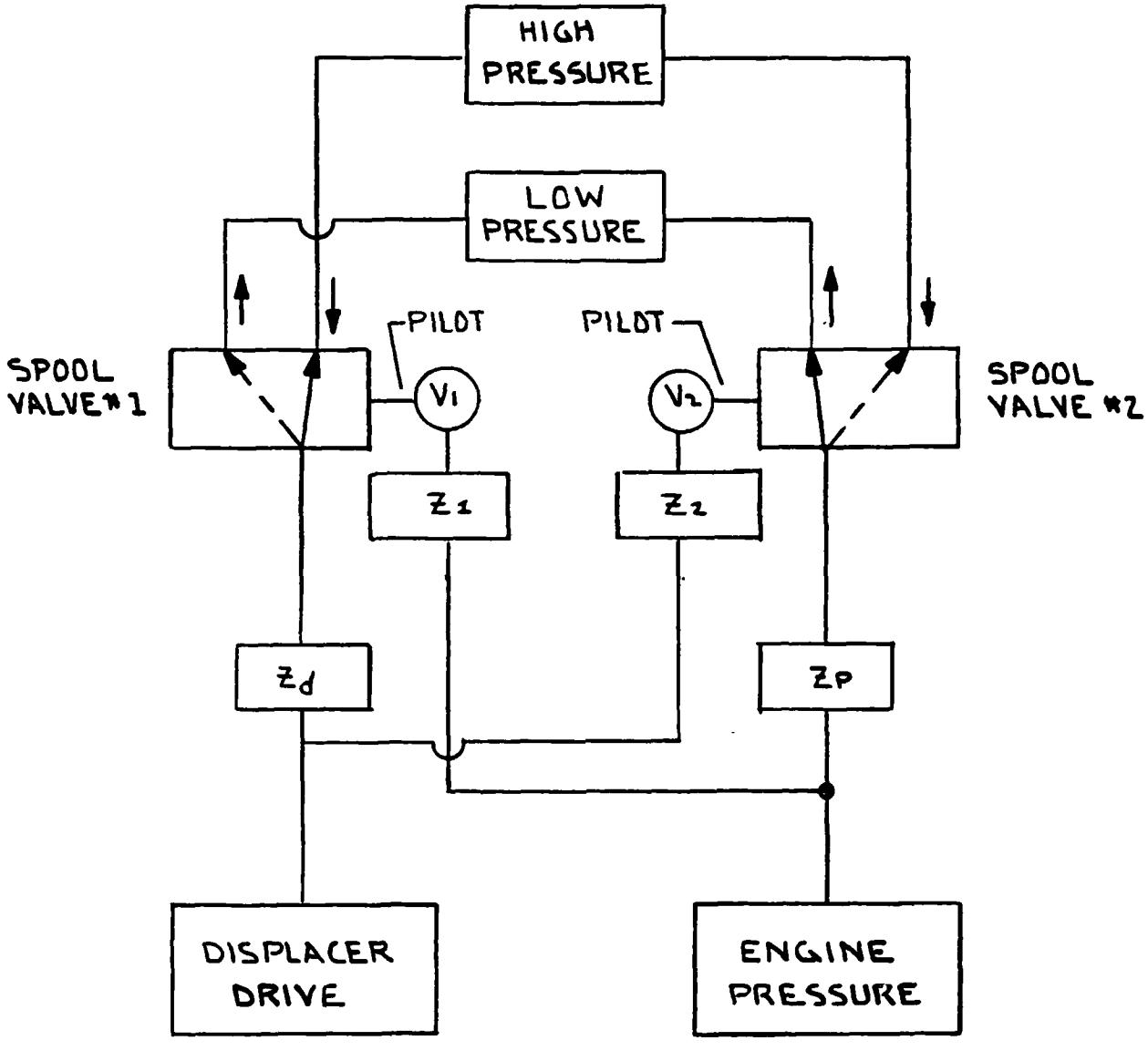

	ENGINE CYCLE	DISPLACER MOTION	ENGINE PRESSURE
1	REGENERATION	DOWN	CONSTANT
2	COMPRESSION	STILL	INCREASING
3	REGENERATION	UP	CONSTANT
4	EXPANSION	STILL	DECREASING

the amount of gas which must be cycled and draw comparisons with commercially available compressor systems.

Accounting for the respective temperatures and volumes of the four stages of the cryocooler, the total molar contents of the machine at the beginning of the expansion process will be about .013 moles of ^3He, which corresponds to about 290 cm^3 at standard temperature and pressure. For a cycle period of 3 seconds, this corresponds to a flow rate of about 4.4 liters/minute (or about .15 ft^3/min). In addition, we must account for the gas flow required to drive the displacer and pneumatic multivibrator, and further allow for leakage of gas past seals between low and high pressure helium volumes.

With appropriate attention to detail in the mechanical design and construction of the pneumatic system we should require a total gas flow less than about 15 liters/min (or about 0.5 ft^3/min). Commercially available compressors (from ITT Pneumotive, for example) can deliver 22 liters/min (.75 ft^3/min) at a pressure of 100 psi using a 1/4 horsepower motor. Unfortunately 115 volt AC, 1/4 horsepower motors typically draw about 4 amperes for a total input power of order 500 watts which is much too high. These compressors however, deliver fifty percent more flow than is reasonably required and further gains might be expected by using a more efficient DC motor. Yet another alternative is to design a more efficient compressor system which could in effect be matched to our specific application to provide the maximum possible operational efficiency.

A significant advantage could be gained if we relax the requirement that no electrical power be used at the cryocooler head. Zimmerman's machine, for example, which uses a motor-driven power piston to provide the expansion and compression of the fluid, consumes only 50 watts of electrical power and reaches 8.5 Kelvin. Unfortunately the introduction of an electric motor at the cryocooler head would effectively destroy the magnetic cleanliness of the machine. The only possible exception might be some type of high frequency induction motor which contains no iron winding forms. Even in this case, however, the device to be cooled would be subject to magnetic fields fluctuating at the characteristic frequency of the motor.

To conclude this discussion, we feel that there should be no significant problem in eventually attaining the goal of 250 watts total input power to the cryocooler. Since it will be desirable in any event to optimize the operation of the cryocooler/compressor combination, we anticipate addressing this problem in detail during the course of the cryocooler work, perhaps even to the extent of designing and building a compressor which is better suited to our needs. As yet however, we have no idea what the final form of the cryocooler will be, and it is premature to try to define the details of a compressor system at this point.

C. Displacer and Cylinder Design

The purpose of a staged cryocooler is twofold. First the decreasing volumes at the lower temperatures compensate for the increasing density of the helium so that each stage has roughly the same molar content during expansion, and secondly the intermediate stages provide thermal sinks at the higher temperatures so that heat can be removed at points where refrigeration is more easily produced. A basic problem in using nylon or similar material for the cylinder and displacer is that as the thermal conductivity of the nylon drops with decreasing temperature it becomes more and more difficult to efficiently use the refrigeration which is produced in the working fluid.

One approach to this problem is to use a segmented cylinder construction in which the cylinder contains metal inserts at each refrigeration stage as shown in Figure 9. This technique allows effective thermal contact between the refrigerant (the working fluid) and the external cylinder walls to provide refrigeration at intermediate stages for electrical leads and thermal shields which are external to the cryocooler.

A significant complication of this construction is that the cylinder must be kept leak tight for internal pressures up to 6 atmospheres and the structure must be able to withstand many, many pressure fluctuations between 1 and 5 atmospheres. The constant fluctuations will probably eliminate the possibility of using any type of plastic-to-metal seal; the alternative is to use some type of soft-metal o-ring (indium, for example) at the cylinder wall joints.

Figure 9. Mechanical Construction of Staged Displacer and Cylinder

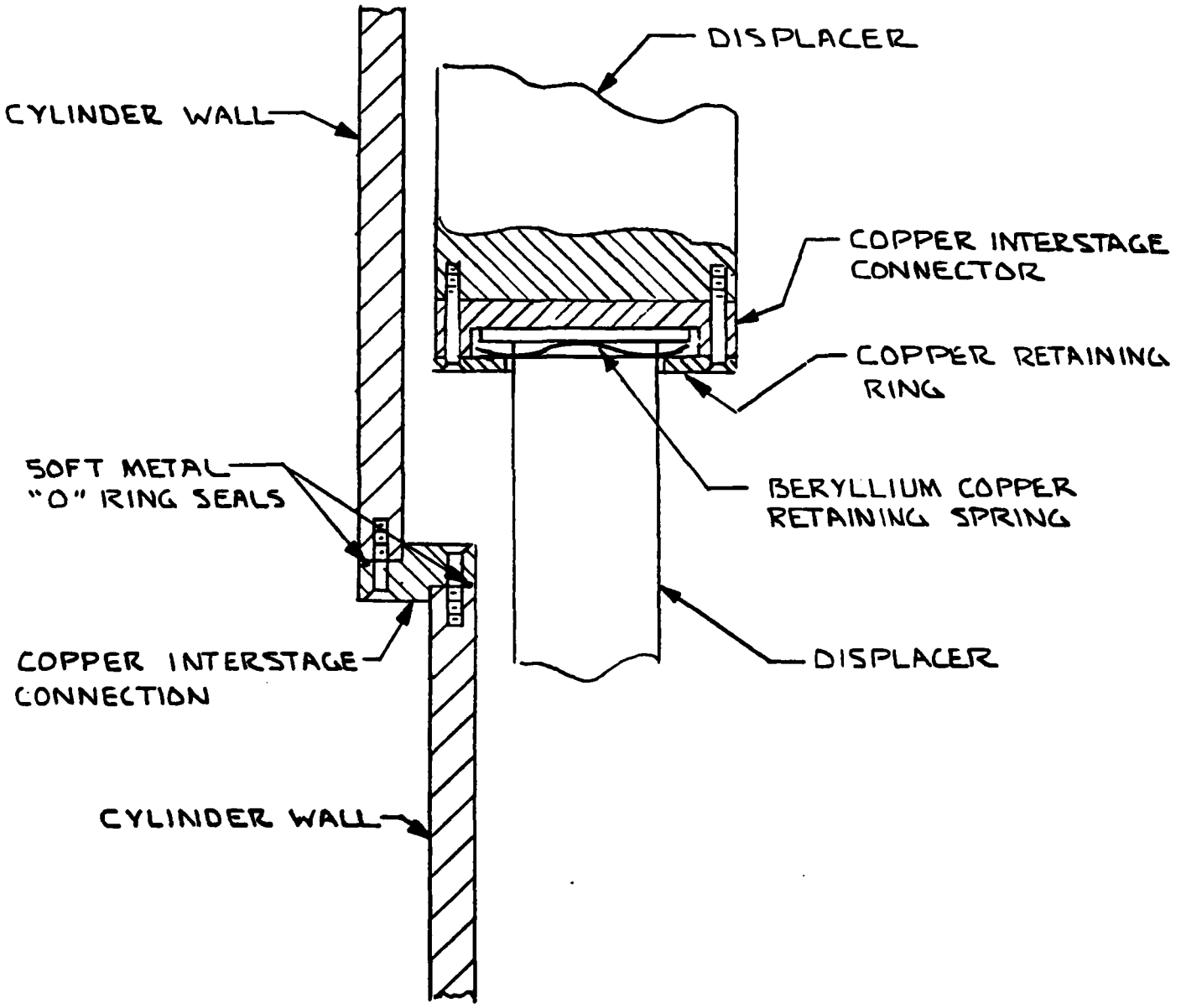

Figure 9 also shows a segmented displacer which allows lateral movement between the stages. For regeneration gaps of order .005 cm the concentricity of successive stages is absolutely essential if the displacer is to move freely and provide a uniform regeneration gap around the cylinder. In practice it will be difficult to construct the cylinder and displacer to that accuracy. To help alleviate the problem we suggest a displacer design as shown in Figure 9 in which each stage of the displacer is held in place longitudinally against the next higher stage by the beryllium-copper spring but can move transversely to align itself with the cylinder.

D. Thermal Coupling to the Cryocooler

Another aspect of the cryocooler's mechanical design we have considered is the problem of efficiently coupling a superconducting device to the refrigeration which is produced inside the cryocooler. The problem arises from the poor thermal conductivity of the helium refrigerant at the lowest anticipated temperatures. For example, at 6K the effective thermal penetration depth in ^{4}He at 6 atmospheres during a period $\tau/4$ is approximately .037 cm for a τ of 3 seconds (and about .050 cm for ^{3}He). This is to be compared with the dimensions of the fourth stage expansion volume which is a cylinder 1 cm in diameter and .6 cm in height. The point is that during the process of expansion and the ensuing regeneration (a total period of 1.5 sec) only 2/ percent of the ^{4}He refrigerant (37 percent for ^{3}He) in the coldest stage will be able to absorb energy from the walls of the expansion volume. The remaining fluid will be significantly colder than the walls of the expansion volume when the regeneration cycle starts and the refrigeration will in effect be used inefficiently at some warmer point in the machine.

Since the effective thermal penetration depth of the helium refrigerant is so small, the solution is to insure that a large percentage of the helium is, at some point, in close contact (of order one thermal penetration depth) with a more highly conductive material. Our suggestion for achieving this condition is to use a metal "cap" on the cold end of the device as shown in Figure 10

Figure 10. Mechanical Arrangement For Thermal Coupling To The Cryocooler

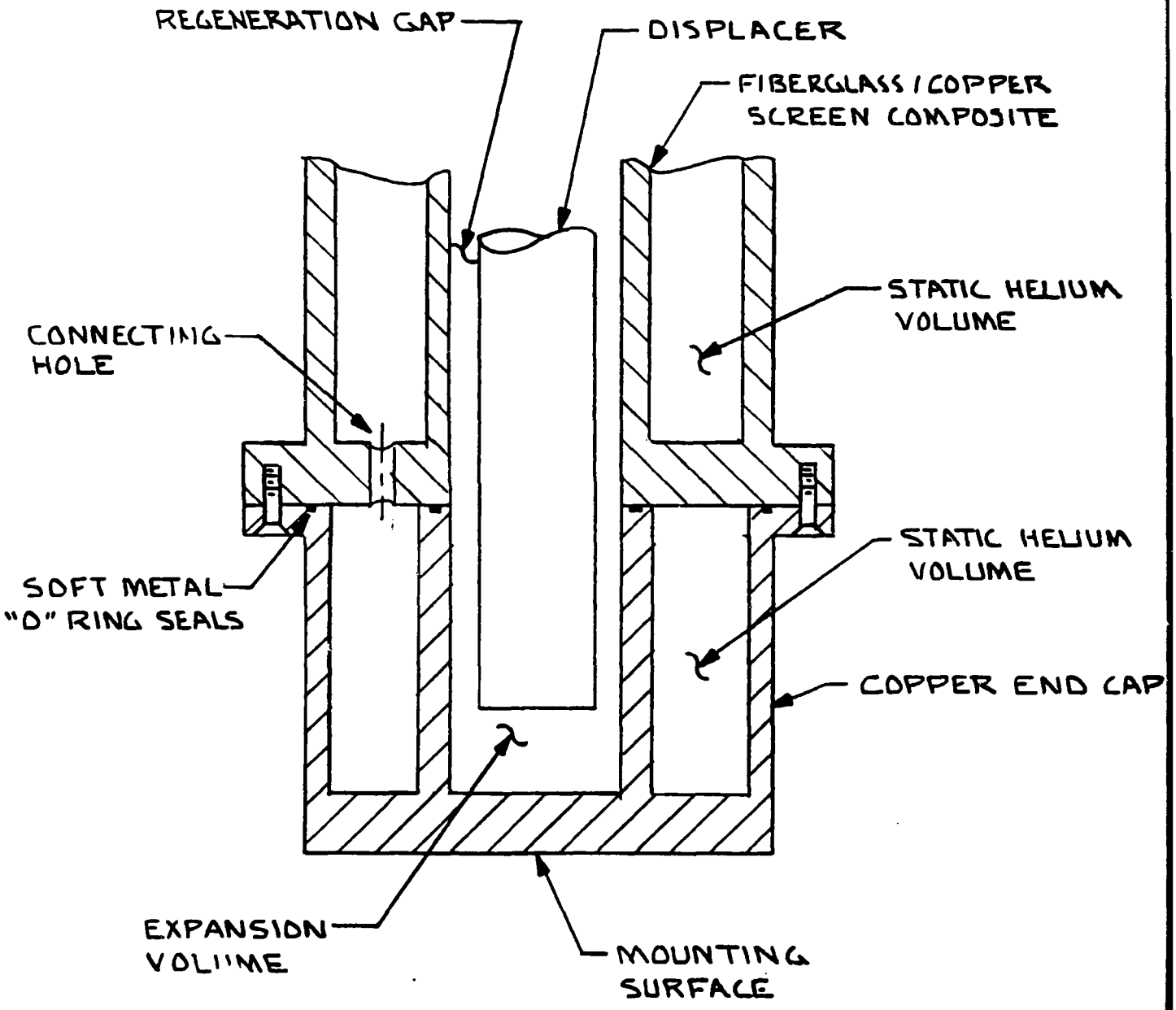

which would effectively extend the regeneration gap of the last stage but would replace the regenerator with a thermally conducting material. Hence during the expansion process and the subsequent regeneration, all of the cold helium leaving the expansion volume would be in close proximity (of order .005 cm) to the thermal load allowing the cold fluid to readily absorb heat from the end cap.

Another feature which we feel is important in the thermal coupling scheme is the provision for additional heat capacity in the thermal load. Refrigeration in the cryocooler is produced in spurts during the expansion portion of each cycle, but between the intervals of refrigeration the expansion volumes will tend to warm as the fluid in the regenerator is compressed and the fluid flowing into the cold end introduces additional heat via regeneration losses. When the cryocooler has reached its lowest temperature, the total cooling produced by the expansion will be just sufficient to offset the warming produced during the rest of the cycle. The net result of these processes will be a temperature fluctuation in the expansion volume at the frequency of the cryocooler cycle which will produce a temperature oscillation in the thermal load. The problem is enhanced by the low heat capacities of materials at liquid helium temperatures.

Our solution, is to provide a large heat capacity in the thermal load in the same manner as in the fourth stage regenerator; that is, by loading the end cap with helium. The helium with its high heat capacity provides a thermal ballast which can absorb the thermal oscillations inherent in the cryocooler cycle. For example, for a 1 cm diameter displacer and a cylinder of outside diameter 3 cm, a solid end cap might contain about 25 cm^3 of copper. If the energy absorbed by the expanding fluid on each cycle is of order .3 joules (100 mwatts with a 3 second period), each expansion process would produce a temperature drop of order 3K (using the heat capacity of copper at 8K of .0042 joules/cm^3-K). A temperature fluctuation of this magnitude will generate a substantial thermal wave in any device which is attached to the exterior of the cryocooler.

However, if we introduce helium at 6 atmospheres into a static volume in the end cap which could easily be of order 10 cm^3 as shown in Figure 10, the

temperature change would be only .04K for the same amount of refrigeration per cycle. With the temperature fluctuations reduced to this level, an appropriate thermal impedance could be used to couple a device to the cryocooler and yet completely isolate it from temperature fluctuations driven by the cryocooler cycle.

The major disadvantage of this technique is that the presence of the helium in the end cap (as well as in the loaded regenerator) will increase the cool down time of the refrigerator. It is not clear that this drawback can be easily avoided since at least some thermal heat capacity is required at the cold end to smooth out temperature fluctuations from the refrigeration cycle. It is possible, of course, for the requisite thermal mass to be contained in the device to be cooled, in which case the helium loaded end cap could simply be replaced with a solid copper cap.

E. Mechanical Vibrations

We anticipate that a major problem in this type of cryocooler design will be mechanical vibrations produced by the oscillating displacer and the cyclical expansion-compression processes. If the final device is longer than 50 cm or so, low frequency vibrations will be effectively amplified by natural resonances of the cylinder which will be attached to a solid support only at its warm end.

To help alleviate this problem we expect to use a technique which was previously developed by S.H.E. Corporation to solve a similar problem in liquid helium dewars. A schematic drawing of the technique is shown in Figure 11. The cryocooler and superconducting instrumentation to be cooled is encased in high resistivity superinsulatin to reduce radiation loss from the room temperature vacuum wall. Three Kevlar cords, attached to the cold-end of the cryocooler, are threaded through the superinsulation out to the surrounding framework where they pass through eyelets, then to the top of the cryocooler to be attached to some simple mechanism for drawing them taught. This construction has several effects. First the taught Kevlar cords provide mechanical support for the cold end of the cryocooler which will be especially important if the device is to be used in a horizontal position. This will undoubtedly be required in many field applications for the device. Another effect of the

Figure 11. Mechanical Support Structure For the Cryocooler

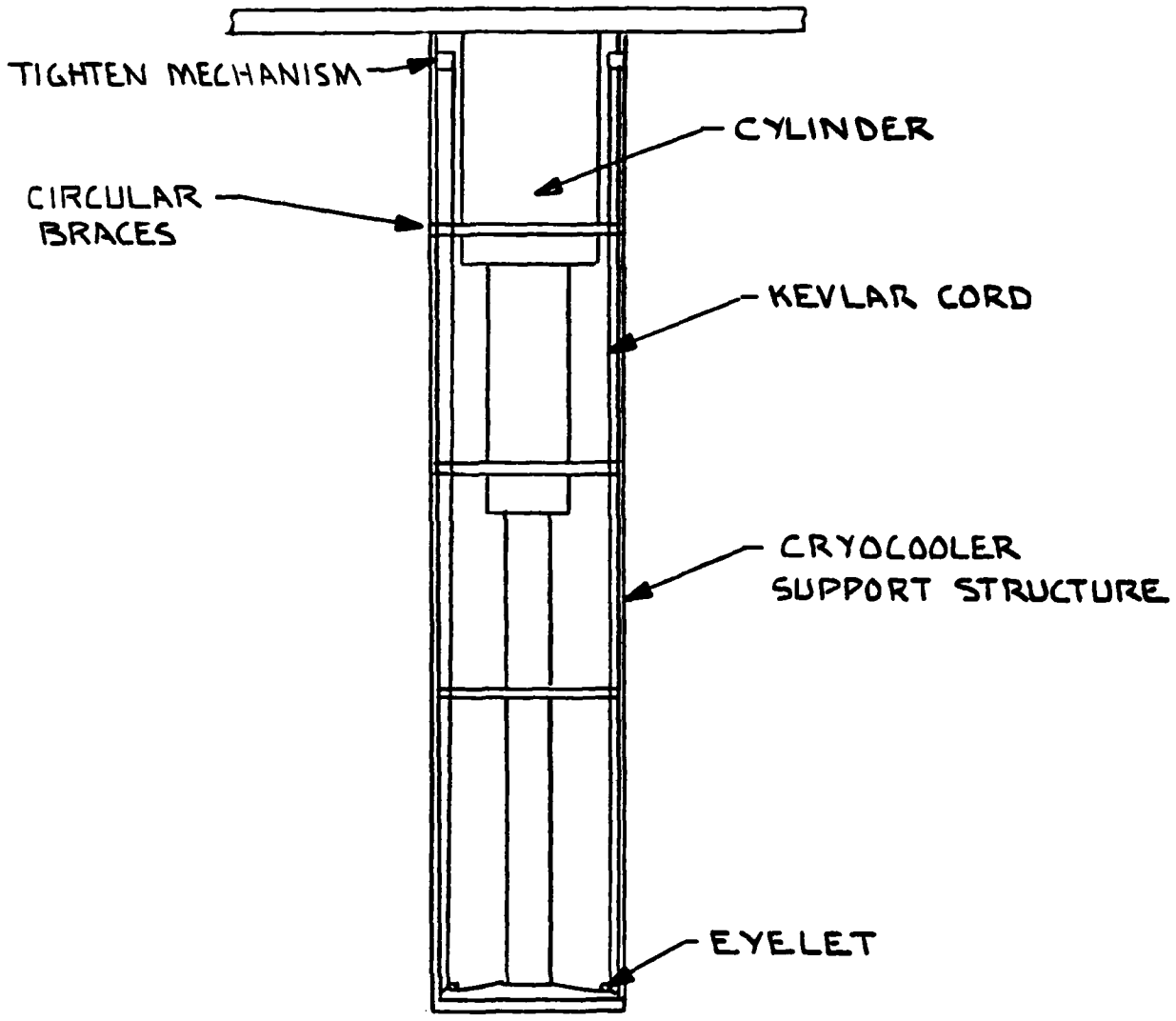

Kevlar cords is to increase the frequency and decrease the amplitude of the natural resonances of the cylinder. Although the resonant frequencies of the cylinder without the Kevlar cords should be substantially above the frequency of the displacer motion and engine cycle, in the absence of significant damping forces enough energy could easily couple to the cylinder resonances to produce unacceptable oscillations. Finally, the cords also provide the requisite damping due to the friction where the Kevlar cords pass through the eyelets.

The primary problem we see with this technique is that a certain amount of care will be required to insure that the cylinder is not pulled out of alignment during the process of tightening the cords. If this presents a significant difficulty we will probably incorporate some type of centering device which could be either permanently installed in the surrounding framework or could be used temporarily while tightening the cords.

IV. MAGNETIC AND VIBRATIONAL CHARACTERISTICS

Three major characteristics of the cryocooler will determine its usefulness for many possible applications: its refrigeration capabilities, its vibrational characteristics, and its magnetic signature. At the end of our development program we will have to have detailed information concerning each of these traits. Since we will be performing constant measurements of the thermodynamic behavior of the machine in attempting to understand the physical processes occuring inside, in the final stages of its development we will have already compiled detailed information on the refrigeration capacity and thermal losses of the cryocooler. The magnetic and vibrational characteristics of the machine, however, will depend on the exact materials and construction techniques used in the final version so these measurements will not be performed until we have a device which meets the thermodynamic requirements.

One of the applications of primary interest for closed-cycle cryocoolers is to cool superconducting devices for use in magnetometry and magnetic gradiometry measurements, hence the magnetic and vibrational signatures of the machine will be of considerable importance. Throughout our preliminary study we have tried to achieve a design which is consistent with low magnetic and vibrational signatures; in the final product we will verify the vibrational and magnetic characteristics of the device through measurements. We anticipate using SQUID sensors to perform the measurements, which is particularly appropriate since SQUIDs are widely used in magnetometry applications where low sensor noise is required. We expect to use several configurations in attempting to isolate the various sources of magnetic noise generated by the cryocooler; similarly, a complete characterization of the vibrational modes of the device will require several measurements.

Our first test will consist of merely scanning the cryocooler while it is operating with an in-house second derivative SQUID gradiometer, which will provide an overall magnetic signature for the instrument. To measure the magnetic characteristics of the machine in more detail, we will need to examine two types of magnetic effect: the induced magnetism in the materials

used in the machine, and the magnetic signals from eddy currents which are induced in conducting materials in the cryocooler due to changes in, or motion through, an ambient magnetic field. The eddy-current signature is particularly important in applications where the cryocooler is to be used on moving platforms, as, for example, in aircraft. We also intend to use SQUID sensors to obtain the vibrational spectrum of the device through mutual inductance measurements. The details of the measurements are presented in the following sections.

A. Magnetic Signature

As mentioned above, we will obtain a first estimate of the overall cryocooler magnetic signature by scanning the cooler while it is operating with a second derivative SQUID gradiometer. The second derivative gradiometer is an in-house instrument designed and built by S.H.E. Corporation which is especially suited to the detection of small magnetic signals from nearby sources. While providing a rough picture of the total magnetic signature of the cooler, this measurement will also help localize the origin of any large magnetic signals being generated within the cryocooler.

A more definitive measurement and much more severe test of the magnetic cleanliness of the cryocooler is shown schematically in Figure 12. In this test we propose to enclose the cryocooler in a specially constructed dewar which will have provision for a liquid helium bath below the cold end of the cryocooler. A SQUID sensor will reside in the helium bath with counterwound sensing loops supported immediately below the end cap of the cooler, around the position which will normally be occupied by a superconducting device attached to the cryocooler. The gradiometer configuration of the sensing loops will decrease the SQUID's sensitivity to the earth's magnetic field, yet allow us to detect magnetic gradients from nearby sources, i.e., the cryocooler. This type of measurement is particularly useful since it will provide direct information on the magnetic fields generated at the position of any device which is to be cooled by the refrigerator. Three successive measurements with the SQUID sensing loops oriented orthogonally during the different measurements will help produce a well defined map of the magnetic environment at the bottom of the cryocooler.

Figure 12. Arrangement For Measuring Vibration and Magnetic Signatures Of The Cryocooler

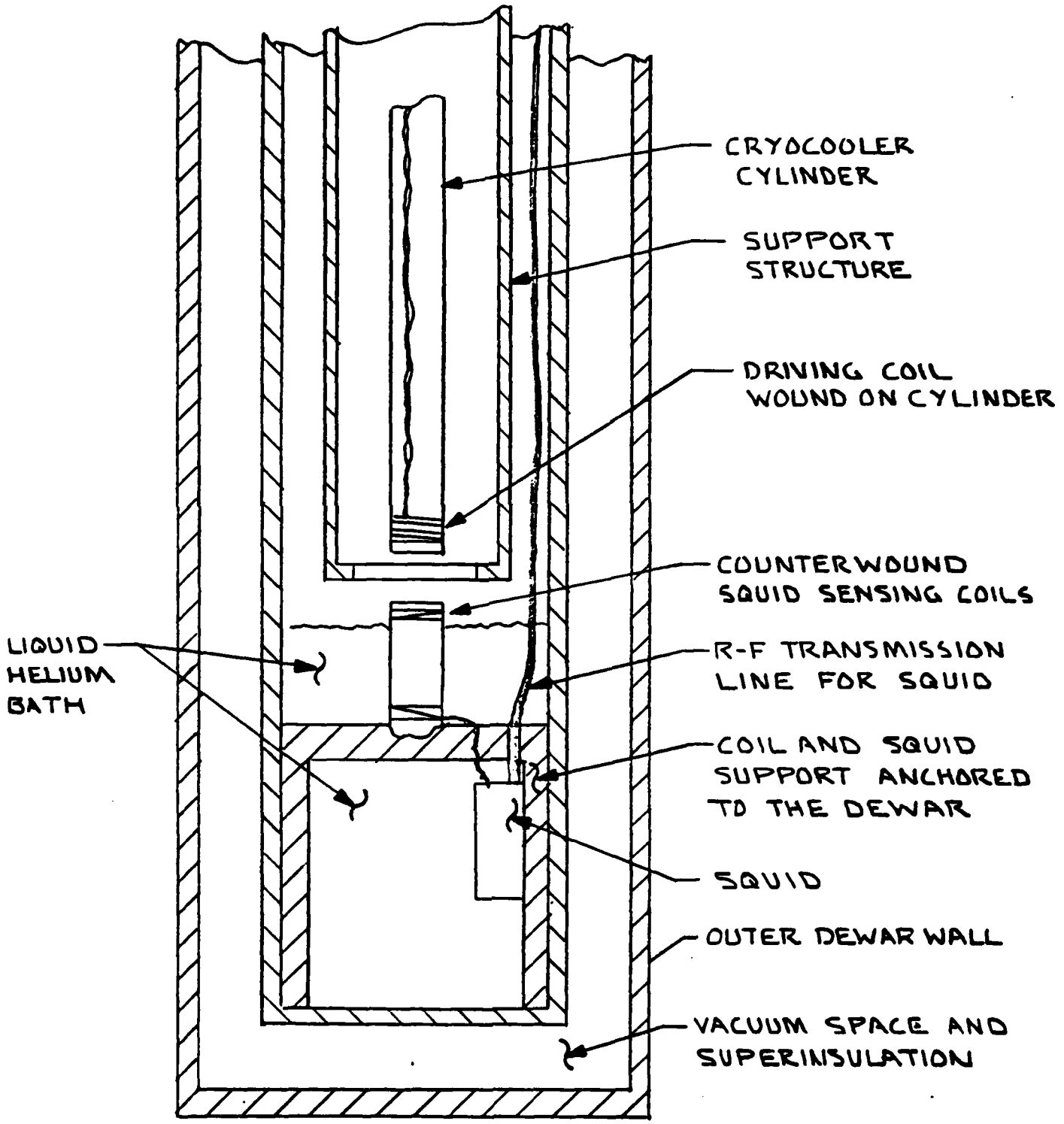

In the same series of measurements we could also obtain information on the eddy current characteristics of the cryocooler by placing the system in an external magnetic field which is oscillating sinusoidally in time. In this configuration, any direct pick up of the external field by the SQUID will appear in the SQUID output as a signal which is in phase with the oscillating field with an amplitude which is independent of frequency. Magnetic fields arising from eddy currents, however, will be 90 degrees out of phase with the driving field and have a magnitude which is frequency dependent. The measurements will not require an especially uniform external field since the in-phase component in the SQUID response can easily be detectd and nulled out using feedback. Again, by performing three successive measurements with the SQUID sensing coils in orthogonal orientations, we can map the magnetic signature of the device which is due to eddy currents.

B. Vibrational Signature

Although the SQUID sensor is essentially a magnetic sensor, we can also use it to obtain vibrational spectra of the cryocooler through mutual inductance measurements. In this type of measurement we use an additional driving coil which is wound directly on the cryocooler. Since the mutual inductance between the driving coil and the SQUID sensing loops is only a function of the coil geometry, any relative motions of the coils appear as a change in their mutual inductance.

Again we use the geometry shown in Figure 12. If we apply a small oscillating current to the driving coil, we will generate a corresponding signal in the SQUID sensor. Using a mutual inductance bridge and phase sensitive detection with the cryocooler not operating, we can estabish a null condition in the SQUID such that the feedback signal to the SQUID exactly cancels the oscillating signal in the SQUID output. If the cryocooler is then turnd on, the SQUID output will fluctuate in response to changes in the mutual inductance between the two coils as the cryocooler cylinder moves. As long as the frequency of the driving signal is substantially higher than the mechanical oscillations of the cryocooler, the output of the SQUID sensor will accurately reflect motions of the cylinder. As with the magnetic signature measurements,

successive measurements with different orientations of the pick up coils can provide information on the oscillatory modes of the engine.

This technique assumes that the SQUID and its sensing coils are rigidly attached to the dewar which in turn is effectively decoupled mechanically from the cryocooler. This should not present a significant problem since the dewar will naturally be rather massive and the upper support of the cryocooler can be securely anchored to an external framework. Another potential complication is that, in addition to the vibrational noise generated in the SQUID, the magnetic signature of the cryocoler will also produce a signal in the SQUID output. However, the mechanical support system we intend to use should raise the natural frequencies of the cryocooler far above the engine frequency of .3 Hz (where the magnetic signature effects will occur), and furthermore, by using the driving signal and narrow band phase sensitive detection, the measurement should exclude effects which are not directly related to the mutual inductance of the driving and pick up coils.

V. CONCLUSIONS

During the course of this work we have examined the basic physical mechanisms which to first order govern the performance of a regenerative cycle cryocooler. From our results in Section II it is clear that regeneration loss is the limiting factor in regenerative coolers operating below about 15 Kelvin, while shuttle and conduction losses dominate in the warmer stages. We also described in Section II how the low-temperature performance of a regenerative cooler might be improved by increasing the regeneration capacity of the coldest stage and by using ^{3}He as the working fluid. From our comparisons with Zimmerman's machine, which has reached 8.5 Kelvin using only plastics (nylon and G-10 fiberglass) as regenerating materials, we feel that the results presented in Section II provide great promise for substantially improving the low-temperature performance of regenerative cryocoolers.

We also wish to emphasize an important point here with regard to the Statement of Work in our proposal. In our original preproposal work we anticipated the possibility that an additional tandem cooling stage operating on a different cycle might be required to reach a temperature of 4 to 5 Kelvin. After performing the analysis in Section II we concluded, however, that the additional stage would not be required, and the time which had been allocated for that investigation was devoted to a more detailed look at the Stirling cycle cooler.

Another aspect we had hoped to investigate in detail is the question of cool down time from start-up. Although our orientation has been toward highly reliable cryocoolers which will remain cold for long periods of time, the initial cool down time is still important, and an excessive cool down time would make the cryocooler unsuitable for some applications. From Zimmerman's work we know that it is desirable to use a longer displacer stroke during start up to reduce the initial cool down time, and this is consistent with our observations in Section II. Specifically, regeneration loss in the colder stages will not become important until the machine approaches its ultimate

temperature, and a longer displacer stroke will increase the refrigeration power of every stage. During the first part of the development program we expect to perform experiments to further define the mechanisms which control the cool down time of the cooler so that we can produce a final device which will have an acceptable performance in this respect.

As we have emphasized throughout the course of this work, we believe that the best approach is a well-organized, systematic effort in which we begin by understanding the basic physical principles involved in a simple single stage machine before proceeding to the more complicated multistage device. To this end we have first examined the physical mechanisms which, to first order, govern the performance of a regenerative cycle cryocooler and the results of those investigations are presented in this report. By viewing the problem from this vantage point we have already gained an appreciation for the factors which fundamentally limit the performance of existing cryocoolers, and the improvement to be expected using our own innovations. Nonetheless, our work to date has been strictly theoretical in nature and has yet to be verified in detail.

The first direct comparison of our calculations with experiment will occur when we have begun measurements on a single stage engine which uses an articulated engine cycle, and only at this point will we actually begin to understand the details of the cryocooler's operation. This consideration has certainly contributed in part to our preference for an articulated engine cycle since we believe that it will be much easier to sort out the individual processes occuring simultaneously in the machine if the engine uses an articulated cycle with a constant displacer velocity rather than a sinusoidal cycle. The same considerations apply to our desire to use helium reservoirs and valves so that the compression and expansion processes can occur at constant pressure with the resulting advantages and simplifications. As a result of using these features in a simple single stage machine, we expect to gain a more precise knowledge of the fundamental processes inside.

The information we derive from a simple machine will be directly applicable to the design of a more complicated multistage machine, and as our learning process continues we expect to continually incorporate new information into

more optimum cryocooler designs. In particular, we anticipate eventually developing a Zimmerman-like machine for applications which do not require such stringent magnetic cleanliness, but which will be smaller and have better low-temperature performance as a result of the knowledge we gain through the current development program.

VI. PROPOSED WORK FOR PHASE II

For the work in Phase II of the cryocooler development program we have essentially two alternatives. The first is to proceed with the development of the entire engine in a systematic fashion starting with a single stage engine working between room temperature and some low temperature of order 150K, understand the processes of cooling and loss which occur in such a simple system, and then advance to the more complicated multistage device. However, since most of our ideas for innovations and the most important part of our calculations deal with the temperature region below 30 Kelvin, an alternate approach is to construct a single stage engine which incorporates our ideas for the lowest temperature stage, and which would operate with its warm end at about 30 Kelvin. This device might then prove or disprove the validity of our ideas.

Our original concept for the cryocooler development program was a staged approach in which we would first build a single stage machine operating from room temperature down to about 150 Kelvin or so. Information and experience gained while constructing and studying this machine could then be applied in building the colder stages and would provide a sound experimental understanding of the refrigeration and thermal loss processes in the machine. In addition, we would then have developed a solid basis from which to approach the much more difficult problem of cooling below 30 Kelvin. Unfortunately, this approach is less desirable from a "proof of principle" standpoint since experimental verification of the real innovations is delayed until nearly the end of the development program.

In view of the time constraints on Phase II (1400 - 1500 man-hours) and the desire to demonstrate the validity of our innovations at some point prior to the final phases of the project, we propose that Phase II consist of a detailed design effort centered on the coldest stage of the cryocooler. It would then be our intent to construct and operate a single stage engine with its warm end at 30 Kelvin during Phase III. The danger in this approach is that we will be attacking the most difficult problem first with very little

experimental background in the operation of mechanical low temperature refrigerators.

The work in Phase II would result in a detailed design for a single stage engine to operate below 30 Kelvin which is intended to be readily adaptable to a complete cryocooler assembly. In addition, the proposed Phase II work will include designing a cryostat suitable for operating and evaluating the performance of the single stage device below 30 Kelvin. Some limited construction and testing may be possible; for example, a preliminary model of the stage should be built to test for its ability to withstand many, many cycles of pressure fluctuation.

The various tasks we propose to undertake during the Phase II work include the following:

1. Develop a detailed design and construction technique for the coldest stage of the proposed cryocooler.

2. Design a suitable cryostat within which a single stage device could operate with its high temperature at about 30 Kelvin.

3. Define specific measurements to be performed, identify the required instrumentation for the measurements, and incorporate the instrumentation into the cryostat and single stage cryocooler designs.

4. Construct a preliminary model for the single stage device and evaluate its ability to withstand expected pressure fluctuations.

5. Develop a detailed mechanical design for thermally coupling a superconducting device to the cold end of the cryocooler.

6. To the extent possible, incorporate the thermal coupling mechanism into the preliminary model of the single stage device and measure the effects of thermal ballast in the coupling mechanism.

We feel that these tasks can be reasonably performed in the proposed time frame and at a level of detail which will allow a straightforward and rapid progression to constructing an actual experiment early in Phase III. Our estimated time frame is shown in Figure 13.

It is important to note that the above list of tasks does not include operating the single stage device as a cryocooler with an oscillating displacer and a fluctuating pressure system. An experiment of this nature will require a substantial investment in time to construct the cryostat and mechanical system which would be required and is clearly beyond the scope of the proposed level of effort for Phase II. Hence we reserve these tasks for Phase III with the comment that such an experiment could probably be in progress within three months after the beginning of Phase III (assuming that a physicist and one technician were both working essentially full time on the project).

At the conclusion of these Phase III experiments (assuming favorable results) we will then be in a position to undertake a detailed design effort for the three stages of the cryocooler to span the temperature range between 30 Kelvin and room temperature. Since various other researchers have successfully built machines which operate over this range, the process should consist more of a learning process with attention to good engineering design rather than a long range innovative research and development project.

Figure 13. Time Chart for Phase II

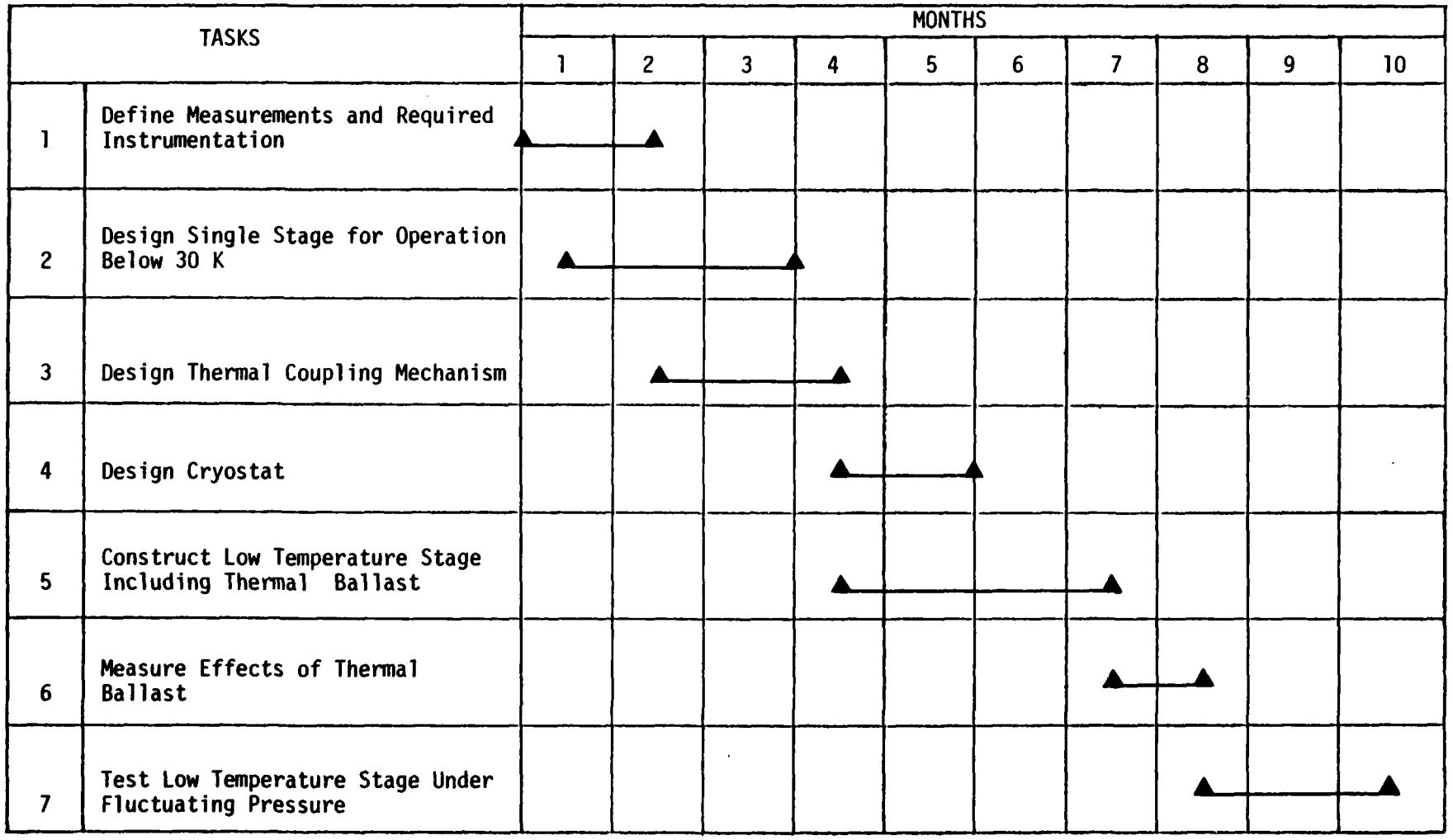

REFERENCES

1. J. E. Zimmerman and Ray Radebaugh, "Operation of a SQUID in a Very Low-Power Cryocooler", NBS Special Publication 508, National Bureau of Standards, 59 (1978).

2. R. Radebaugh and J. E. Zimmerman, "Shuttle Heat Transfer in Plastic Displacers at Low Speeds", NBS Special Publication 508, National Bureau of Standards, 68 (1978).

3. L. Monchick, E. A. Mason, R. J. Munn, and F. J. Smith, Phys. Rev. 139, A1076 (1965).

4. F. J. Zimmerman and R. C. Longsworth, Adv. Cryog. Eng. 16, 342 (1970).

APPENDIX A
REGENERATION LOSS

In a Stirling cycle cryocooler the working fluid is moved back and forth between the hot and cold ends of the machine and refrigeration is produced by isothermally compressing the fluid while it is in the hot end of the cooler and expanding the fluid while it is in the cold end. In moving from the hot end to the cold end the fluid will tend to give up heat to its relatively colder surroundings, and the effect will be reversed when moving from the cold to the hot end. This process is called regeneration and ideally as the fluid moves it will remain in thermal equilibrium with the machine.

In fact, of course, the process is not ideal and the fluid will arrive in the cold end of the machine at some slightly greater temperature than the machine itself. The resulting transport of heat into the cold parts of the machine represents a thermal load on the machine and is referred to as regeneration loss. We wish to compute this effect for a machine in which the displacer cycle consists of four discreet motions: (1) a constant velocity hot-to-cold regeneration; (2) fluid expansion during which the displacer is stationary; (3) a constant velocity cold-to-hot regeneration; and (4) fluid compression during which the displacer is again stationary.

During the hot-to-cold regeneration the wall temperature at the surface of the regeneration gap will increase as the wall absorbs heat from the fluid, then during the ensuing expansion the wall surface temperature will drop back toward some equilibrium temperature as the absorbed heat diffuses further into the wall and as the fluid begins to reabsorb heat. In the following cold-to-hot regeneration the wall temperature will be driven below its equilibrium temperature as the low pressure fluid is regenerated to room temperature, then relax back toward its average temperature as the fluid is once again compressed. We model the problem as follows.

Since the engine cycle is not sinusoidal, the most general solution to the problem will entail solving the complete heat flow equation in a cylindrical geometry with non-sinusoidal, time-dependent boundary conditions. Furthermore since there are other thermal processes occuring simultaneously such as

viscous heating and shuttle heat transfer, the general solution is an extremely complex problem.

To construct the problem we first consider a narrow annular gap of diameter D and width d as shown in Figure A-1, where d << D so that the cross-sectional area is approximately πDd . If fluid flows through the gap with laminar flow, the fluid velocity is given by:

$$\vec{v} = \frac{3}{2} \bar{v} \left(1 - \frac{4r^2}{d^2}\right) \hat{z} \qquad \text{(A-1)}$$

where $\bar{v}$ is the average fluid velocity across the gap, r is measured from the center of the gap, and the velocity is zero at the walls. The heat flow equation is

$$\frac{\partial T}{\partial t} + \vec{v} \cdot \text{grad } T = \kappa \nabla^2 T \qquad \text{(A-2)}$$

where $\kappa = K_f/\rho C_p$ is the thermal diffusivity of the fluid, K_f is its thermal conductivity and ρC_p is its heat capacity per unit volume. For a steady state system in which the fluid velocity is constant in time, equation (A-2) becomes

$$\frac{\partial^2 T}{\partial r^2} = \frac{3\bar{v}}{2\kappa} \left(1 - \frac{4r^2}{d^2}\right)(\text{grad } T)_z \qquad \text{(A-3)}$$

If we assume that regeneration occurs at both walls, we can integrate equation (A-3) with the boundary conditions $T = T_w$ at $r = \pm d/2$, and $\frac{\partial T}{\partial r} = 0$ at $r = 0$ to get:

$$T_f - T_w = \frac{3\bar{v}}{2\kappa} (\text{grad } T)_z \left[\frac{r^2}{2} - \frac{r^4}{3d^2} - \frac{5d^2}{48} \right] \qquad \text{(A-4)}$$

where T_f is the fluid temperature and T_w is the wall temperature. In what follows we let the subscripts w and f refer to walls and fluid respectively.

Consequently, due to the temperature difference between the fluid and walls, there will be a net transport of heat parallel to the fluid velocity given by:

$$\dot{Q} = \pi D \rho C_p \int_{-d/2}^{d/2} v(r) \, (T_f - T_w) dr \qquad \text{(A-5)}$$

Figure A-1. Laminar Flow In A Regeneration Gap

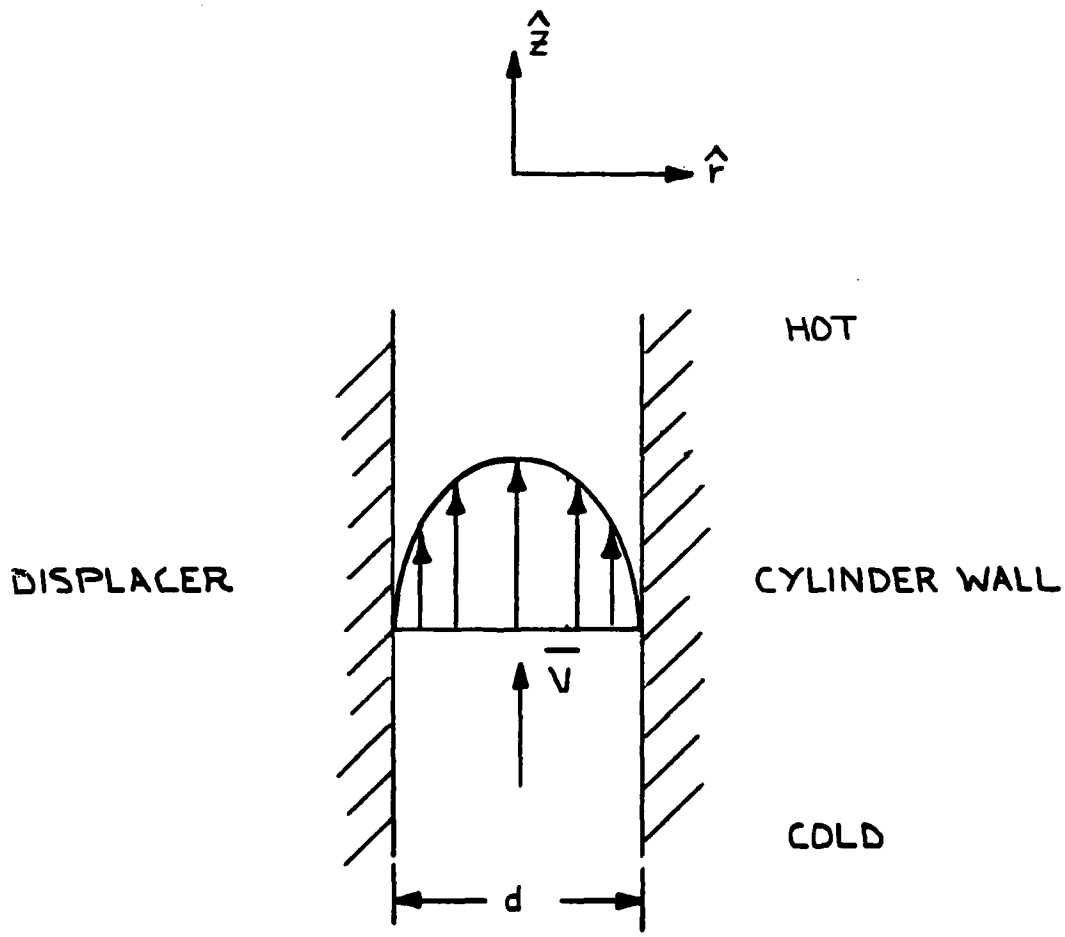

Using equations (A-1) and (A-4) for $\upsilon(r)$ and $(T-T_w)$ respectively, we find

$$\dot{Q} = -\left(\frac{17}{140}\right)\left(\frac{d}{\pi DK_f}\right)\left(\dot{n}_o MC_p\right)^2 (\text{grad } T)_z \qquad \text{(A-6)}$$

where we have used the relationship between the flow velocity υ, and the molar flow rate, $\dot{n}_o$, given by:

$$\upsilon = \dot{n}_o M/\pi Dd\rho \qquad \text{(A-7)}$$

where M is the gram-molecular weight of the fluid. Equation (A-6) represents the thermal transport which results from the finite thermal conductivity of the working fluid, and we note that the regeneration loss is proportional to the square of both the molar flow rate and the heat capacity of the fluid and is inversely proportional to its thermal conductivity.

Note also that in assuming a constant wall temperature, we implicitly assumed an infinite heat capacity in the walls. In other words, we assumed that the walls could absorb heat with no increase in temperature. For any real situation, of course, the temperature of the walls will increase as they absorb heat which will result in additional regeneration losses. To account for the effect of diffusive walls we argue as follows.

In any diffusive medium a thermal wave will propogate according to the heat flow equation given in equation (A-2) with a wavelength, λ, given by:

$$\lambda = \sqrt{2\pi T\kappa} \qquad \text{(A-8)}$$

where T is the period of the wave and κ is the thermal diffusivity of the material. Physically this means that during a period, T, following a change in temperature at the wall, the increased energy flowing into the wall will have penetrated only a distance of order λ. Since the entire regeneration process occurs during a period $\tau/4$ where τ is the period of the engine cycle, we assume that all of the heat of regeneration flows into or out of one "thermal skin depth" given by:

$$\lambda = \sqrt{\pi\tau\kappa/2} \qquad \text{(A-9)}$$

and that within this layer the temperature increases or decreases roughly linearly in time during the regeneration. Hence the heat flow per unit length into the regenerator will be:

$$\dot{Q}_w/L = C_w \pi D \lambda \dot{T} \tag{A-10}$$

where C_w is the heat capacity per unit volume of the walls and D is the diameter of the annular gap. Furthermore, the heat flow per unit area (heat flux) at the boundary is given by:

$$\dot{Q}_w/\pi DL = -K_F \left[\frac{\partial T_f}{\partial r}\right]_{d/2} = -\left(\frac{K_f d}{2\kappa_f}\right) \upsilon(z,t)(\text{grad } T)_z \tag{A-11}$$

so combining equations (A-10) and (A-11) and integrating we find

$$T_w - T_o = \left(\frac{K_f d}{2\kappa_f C_w \lambda}\right) (\text{grad } T)_z \int_o^t \upsilon(z,t')dt' \tag{A-12}$$

where T_0 is some average temperature of the wall, $\upsilon(z,t')$ is the time-dependent fluid velocity along the gap, and t' is a variable of integration. If we now insert equation (A-12) into equation (A-5) to find the thermal transport along the regeneration gap, we can perform the integrations and find:

$$\dot{Q} = -\left(\frac{17\pi D d^3}{140 K_f}\right)(\rho C_p)^2 (\text{grad } T)_z \upsilon^2(z,t)$$
$$\times \left[1 + \frac{70}{17}\sqrt{2/\pi}\ \frac{K_f}{d\sqrt{K_w C_w \tau}}\ \frac{1}{\upsilon} \int_o^t \upsilon(z,t')dt'\right] \tag{A-13}$$

Hence, to find the average regeneration loss we need only determine the time dependence of the fluid velocity in the regeneration gap and then average equation (A-13) over one engine cycle.

We first consider the mathematically simpler case of constant pressure regeneration, and we restrict our discussion to a single stage device in which the maximum volumes at the cold and hot ends are equal, and where subscripts 1 and 2 refer respectively to the hot and cold ends of the engine. Furthermore we consider only hot-to-cold regeneration where the initial volume of the hot and cold ends are respectively V_0 and zero. From the equation of state for an ideal gas the molar contents of the cold end will be:

$$n_z = P_0 V_2 / RT_2 \qquad \text{(A-14)}$$

where P_0 is the pressure at which regeneration occurs, T_2 and V_2 are the temperature and volume of the cold end respectively, and R is the gas constant. Since T_2 and P_0 are constant, the molar flow rate into the cold end will be just proportional to $\dot{V}_2$, which is constant for a constant displacer velocity. Furthermore, the density of the gas, n_2/V_2 is constant and since the molar flow rate is related to the fluid velocity by equation (A-7), v(z,t) must be also independent of time. The integrals in equation (A-13) are now trivial and using equation (A-7) we find:

$$\langle \dot{Q}_R \rangle = \left(\frac{17}{280}\right) \left(\frac{d}{\pi D K_f}\right) (C_p \dot{M} \dot{n}_o)^2 \, (\text{grad } T)_z \times \left[1 + \left(\frac{35}{34}\right) \sqrt{2/\pi} \, \frac{K_f}{d} \, \sqrt{\tau / K_w C_w}\right] \qquad \text{(A-15)}$$

which is our standard equation for regeneration loss when regeneration occurs at both walls.

The other case we wish to consider is that in which the regeneration occurs with the total amount of gas in the engine constant. Since the total volume of the engine is constant and the average temperature of the gas decreases the pressure in the engine will drop as the regeneration proceeds. To begin, we differentiate the ideal gas equation for both hot and cold ends of the engine to get:

$$\dot{P} V_1 + P \dot{V}_1 = \dot{n}_1 R T_1 \qquad \text{(A-16a)}$$

$$\dot{P} V_2 + P \dot{V}_2 = \dot{n}_2 R T_2 \qquad \text{(A-16b)}$$

and we note that since both the total engine volume and the total moles of working fluid are constant:

$$\dot{n}_2 = -\dot{n}_1 \quad , \quad \dot{V}_2 = -\dot{V}_1 \qquad \text{(A-17)}$$

Using equation (A-17) in equations (A-16) and integrating we find that the pressure in engine has the form:

$$P = \frac{P_0 T_2 V_0}{T_2 V_0 - V_2(T_2 - T_1)} \tag{A-18}$$

where P_0 and V_0 are respectively the initial pressure and total volume in the engine. We can write equation (A-18) in reduced form as

$$P' = \frac{T'}{T' + V'(1-T')} \tag{A-19}$$

where $V' = V_2/V_0$, $P' = P/P_0$, and $T' = T_2/T_1$. Note that all the normalized quantities have values between zero and one. Using equation (A-19) in equation (A-16b) we find the molar flow rate at the cold end of the engine to be:

$$\dot{n}_2 = n_0 \dot{V}' \, P'^2/T' \tag{A-20}$$

where n_0 is the total molar content of the engine and $\dot{V}' = \dot{V}_2/V_0$ is the normalized rate of displacement. Note that during the first half of the regeneration the molar flow rate is much higher than during the last part. Now to find the velocity of the fluid along the regeneration gap we need the fluid continuity equation in the gap:

$$\frac{\partial \rho}{\partial t} + \rho \, \vec{\nabla} \cdot \vec{v} + \vec{v} \cdot \vec{\nabla} \rho = 0 \tag{A-21}$$

and we note that the density of the gas is given by:

$$\rho(z,t) = \frac{MP(t)}{RT(z)} \tag{A-22}$$

where the pressure, P(t), is only a function of time, and the temperature of the gas T(z) depends on its position along the displacer. We also assume that temperature differences across the gap will be negligible compared to those parallel to the fluid flow so we can ignore density gradients across the gap. Then differentiating equation (A-21), substituting into equation (A-22), and integrating with the appropriate boundary conditions, we find

$$v(z,t) = \left(\frac{\dot{V}'P'}{T'}\right)\left(\frac{n_0 M}{D\pi d\rho_0}\right)\left[\frac{T(z)}{T'}\right] \tag{A-23}$$

where ρ_0 is the fluid density at the beginning of the regeneration, M is the gram-molecular weight of the fluid, and we have again used equation (A-7) which relates the molar and volume flow rates.

Since the displacer moves with constant velocity, $\dot{V}_2 = 2X_0/(\tau/4)$, the time dependence in equation (A-23) is contained entirely in the factor P' as given by equation (A-18). Using this expression for $\upsilon(z,t)$ we can now integrate equation (A-13), and after some careful algebra we find that the regeneration loss for this case is given by the rather formidable expression:

$$\langle \dot{Q}_R \rangle = (.0204)\left(\frac{d}{\pi D K_f}\right)(C_p \dot{M} n_o)^2 (\text{grad } T)_z \; F(T')$$

$$\times \left[1 + (.616)\left(\frac{K_f}{d}\right)\sqrt{\tau/K_w C_w}\; G(T')\right] \qquad \text{(A-24)}$$

where $T' = T_2/T_1$ and

$$F(T') = 1 + T' + 1/T' \qquad \text{(A-25a)}$$

$$G(T') = \frac{1 - T'(1+2\,\text{Ln}T')}{(1-T')^2(1+T'+1/T')} \qquad \text{(A-25b)}$$

Comparing equation (A-24) with the expression for constant pressure regeneration we note that the function F(T') is just replaced by a constant factor of 3 and $F(T') > 3$ for $T' < 1$, so that constant pressure regeneration will always have a smaller regeneration loss. The problem becomes particularly acute as T' becomes small and F(T') is dominated by the 1/T' term. In the more general case of a multistage engine the functions F(T') and G(T') are complicated functions of both the temperatures and volumes of the various stages but the overall effect is essentially the same.

To understand the effect consider a single stage operating between 150K and 300K. Since the ratio of the molar contents of the hot and cold end is given by:

$$n_{2/n_1} = T_1 V_2 / T_2 V_1 \qquad \text{(A-26)}$$

when the hot and cold volumes are equal (the displacer is half way through its stroke), two-thirds of the gas will already be regenerated. As the cold end

temperature decreases the effect becomes more severe even in a multistage engine with decreasing volumes in the colder stages. For example, in our proposed design (see Table 1 in Section II.G) 82 percent of the fluid would be regenerated during the first half of the displacer stroke.

The last point we wish to examine is the case in which regeneration occurs at only one surface of the regeneration gap. For this situation we return to equation (A-3) in which the boundary conditions now become $T = T_w$ at $r = d/2$ and $-K_f \left(\frac{\partial T}{\partial r}\right) = 0$ at $r = -d/2$. Integrating equation (A-3) with these boundary conditions gives the result:

$$T - T_w = \left(\frac{3\bar{v}}{2\kappa}\right) (\text{grad } T)_z \left[\frac{r^2}{2} - \frac{r^4}{3d^2} + \frac{dr}{3} - \frac{13d^2}{48}\right] \qquad \text{(A-27)}$$

The rest of the analysis is exacty analogous to that for regeneration at both surfaces, and the final result has exactly the same functional form. Hence the final expression for constant pressure regeneration loss is:

$$\langle \dot{Q}_r \rangle = (.186)\left(\frac{d}{\pi D K_f}\right)(C_p \dot{M} n_o)^2 (\text{grad } T)_z \left[1 + .269 \frac{K_f}{d} \sqrt{\tau / K_w C_w}\right] \qquad \text{(A-28)}$$

and we note that the only difference between this expression and equation (A-15) for regeneration at both surfaces is a constant factor of about 3 in the first term.

APPENDIX B
SHUTTLE HEAT LOSS

Shuttle heat occurs through the mechanical oscillations of the displacer. When the displacer is toward the warm end of the engine, each point along the displacer will be somewhat colder than the cylinder wall immediately across the fluid gap, and heat will flow across the fluid gap from the cylinder wall into the displacer. When the displacer subsequently moves toward the cold end of the engine, the situation will be reversed and heat will flow out of the displacer and back into the cylinder wall. The result is a net flow of heat into the cold end of the cryocooler, and the resulting loss is referred as shuttle heat loss.

As with regeneration loss we assume that only one penetration depth, λ, given by

$$\lambda = \sqrt{\pi\tau\kappa/2} \tag{B-1}$$

of the cylinder wall and displacer participates in the shuttle heat mechanism during a period of $\tau/4$. We also assume that during the regeneration process the shuttle heat mechanism will be overwhelmed by the much larger heat of regeneration. Figure B-1 shows the geometry where z_0 is some fixed point on the cylinder, X represents the distance of the displacer from its average position, and X_0 is its maximum displacement. The temperature of the displacer at point z_0 is then given by:

$$T_d(z_0) = \bar{T} + X(\text{grad } T)_z - T_s(t) \tag{B-2}$$

where $\bar{T}$ is the average temperature of the displacer at z_0, $(\text{grad } T)_z$ is the temperature gradient along the gap, and $T_s(t)$ gives the time dependent temperature fluctuations due to shuttle heat transfer. Note that the term X $(\text{grad } T)_z$ arises from the motion of the displacer. Similary, the temperature of the cylinder wall at z_0 is:

$$T_w(z_0) = \bar{T} + T_s(t) \tag{B-3}$$

Figure B-1. Geometry Of Shuttle Heat Transfer

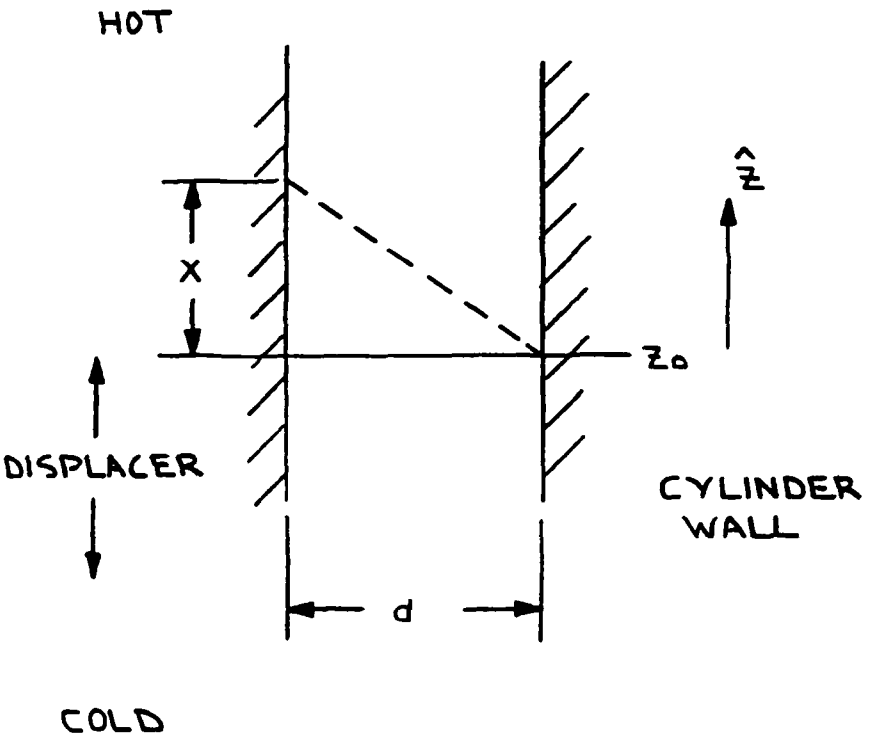

so that temperature gradient <u>across</u> the gap at position z_0 is:

$$T_d - T_w = X(\text{grad } T)_z - 2T_s(t) \tag{B-4}$$

This temperature gradient will drive a heat flow across the gap given by:

$$\langle \dot{Q} \rangle / L = \frac{\pi D K_f}{d} (T_d - T_w) \tag{B-5}$$

where $\langle \dot{Q} \rangle / L$ is the heat flowing into the displacer per unit length, K_f is the thermal conductivity of the fluid, D is the diameter of the annular gap, and d is the size of the gap. If all of the heat flows into one thermal penetration depth of the displacer, the temperature increase of the displacer will be approximately given by:

$$\dot{T}_s = \left(\frac{K_F}{d\lambda C_d}\right) (T_d - T_w) \tag{B-6}$$

and using equation (B-4) we find:

$$\dot{T}_s(t) + 2\alpha T_s = \alpha X_o (\text{grad } T)_z \tag{B-7}$$

where:

$$\alpha = K_f / d\lambda C_d = (K_f/d) \sqrt{2/K_d C_d \pi \tau} \tag{B-8}$$

Integrating this equation with the boundary condition $T_d(t = 0) = \bar{T} + X_0 (\text{grad } T)_z$ we get:

$$T_s(t) = \left(\frac{X_0}{2}\right)(\text{grad } T)_z (1 - e^{-\alpha\tau/2}) \tag{B-9}$$

Now the heat flow along the displacer due to the shuttle heat effect is contained in one thermal penetration depth so that the shuttle heat loss is just given by:

$$\langle \dot{Q}_s \rangle = \frac{1}{\tau} \int_0^\tau (C_d \pi \lambda) T_d \upsilon dt \tag{B-10}$$

where υ is the displacer velocity. Performing the integration with the appropriate boundary conditions and noting that the displacer is stationary during the expansion and cmpression processes we find:

$$\langle \dot{Q}_s \rangle = (\frac{2}{\tau})(\pi C \lambda D X_o^2)(\text{grad } T)_z (1-e^{-\alpha\tau/2}) \qquad \text{(B-11)}$$

and λ is given in equation (B-1). There are two limiting cases which are of some interest. Specifically, if $\alpha\tau << 1$, we have the limiting form

$$\langle \dot{Q}_s \rangle = (\frac{\pi D K_f}{d}) X_o^2 (\text{grad } T)_z \qquad \alpha\tau << 1 \qquad \text{(B-12)}$$

and if $\alpha\tau >> 1$, we have:

$$\langle \dot{Q}_s \rangle = (D X_o^2) \sqrt{2\pi^3 K_d C_{d/\tau}} \ (\text{grad } T)_z \qquad \alpha\tau >> 1 \qquad \text{(B-13)}$$

Equation (B-12) corresponds to having a large heat capacity and thermal conductivity in the displacer which dominates the shuttle heat loss. In the other case, the thermal conductivity and heat capacity of the displacer are small so that the limiting factor in the shuttle heat mechanism is the thermal conductivity of the fluid and the width of the gap.

APPENDIX C
VISCOUS LOSSES

Viscous losses occur in the narrow regeneration passages of the cryocooler, and in the upper stages where there is a large molar flow rate and the viscosity of the fluid is relatively greater, the viscous heating can be significant. To estimate the effect we proceed as follows.

The flow of a viscous fluid through a small gap of width, d, is driven by a pressure gradient $\frac{dP}{dz}$ given by:

$$\frac{dP}{dz} = \frac{12\eta}{d^2}\, v(z) \qquad \text{(C-1)}$$

where η is the coefficient of viscosity, and $v(z)$ is the velocity of the fluid in the gap. If A is the cross sectional area of the gap, then the rate of viscous heating per unit length will be:

$$\dot{V}_r \frac{dP}{dz} = \frac{12A\eta}{d^2}\, v^2(z) \qquad \text{(C-2)}$$

where $\dot{V}_r$ is the volume flow rate of the fluid in the regenerator. The viscous heating can now be calculated from:

$$\dot{Q}_v = \dot{V}_r P = \frac{12A}{d^2} \int_0^L \eta v^2(z)\, dz \qquad \text{(C-3)}$$

Now the molar flow rate, and the fluid velocity and density are related by:

$$\dot{n}(z) = \frac{A}{M}\, v(z)\rho(z) \qquad \text{(C-4)}$$

where M is the gram-molecular weight of the fluid and $A = \pi Dd$ for a small annular gap. But in constant pressure regeneration, the molar flow rate is independent of position so if n_0 is the total number of moles to be regenerated during a period, $\tau/4$, we have, $\dot{n} = 4n_0/\tau$ and:

$$\dot{Q}_v = \frac{12M^2}{d^2 A} \int_0^L \frac{\eta \dot{n}^2}{\rho^2(z)}\, dz = \frac{192(n_0 M)^2}{d^3 \pi D} \int_0^L \frac{\eta}{\rho^2(z)}\, dz \qquad \text{(C-5)}$$

And finally, using:

$$dT = (\text{grad } T)_z \, dz \tag{C-6}$$

we change the variable of integration to get:

$$\dot{Q}_s = 192 \left(\frac{n_o^2 M^2}{\pi D d^3}\right) [(\text{grad } T)_z]^{-1} \int_{\Delta T} \frac{\eta}{\rho^2(T)} \, dT \tag{D-7}$$

The viscous loss is now found by averaging over one engine cycle, but during the compression and expansion processes the flow rate will be small compared to that during the regeneration processes, and during cold-to-hot regeneration viscous heat will be carried toward the hot end of the engine and will not represent a thermal load on the device. Consequently we find the viscous loss to be given by:

$$\langle \dot{Q}_s \rangle = 48 \left(\frac{n_o^2 M^2}{\pi D d^3}\right) [(\text{grad } T)_z]^{-1} \int_{\Delta T} \frac{\eta}{\rho^2} \, dT \tag{C-8}$$

If the density and viscosity are known as a function of temperature, this expression is easily evaluated to yield the viscous loss for each stage of the engine.


DATE
FILME
8